Aligned representation of visual and tactile motion directions in hMT+/V5 and fronto-parietal regions

Authors: Iqra Shahzad[1], Ceren Battal[1], Filippo Cerpelloni[1,4], Alice Van Audenhaege[1], André Mouraux[1], Olivier Collignon[1,3]

Affiliations:

(1) Institute of Neuroscience (IoNS) and of Psychology (IPSY), UCLouvain, Belgium
(2) Brain and cognition, Leuven Brain Institute, KU Leuven, Belgium
(3) The SENSE brain innovation and research centre, Lausanne, Switzerland.

Correspondence should be addressed to: Iqra Shahzad (iqra.shahzad@uclouvain.be) and Olivier Collignon (olivier.collignon@uclouvain.be).

Competing interests: The authors declare no competing interests.

Acknowledgements: We would like to express our gratitude to Dr. Rémi Gau and Dr. Mohamed Rezk for their guidance on data management and analyses and insightful discussions. fMRI data was acquired at the Cliniques Universitaires Saint-Luc (UCLouvain – Université Catholique de Louvain).

Funding:

IS was funded by the European Union's Horizon 2020 research and innovation program under the Marie Skłodowska-Curie grant agreement No 86011 (multiTOUCH). The project was funded in parts by a Mandat d'Impulsion Scientifique awarded to OC, the Belgian Excellence of Science (EOS) program (Project No. 30991544) awarded to OC, and a Flagship ERA-NET grant SoundSight (FRS-FNRS PINT-MULTI R.8008.19) awarded to OC. OC is a senior research associate at the Belgian National Fund for Scientific Research (FRS-FNRS).

Author contributions:

Conception and design: IS, AM, OC

Participant Recruitment: IS

Data Collection: IS, CB, FC, AA

Data Analysis: IS analyzed data under the supervision of OC. CB provided support on data analysis scripts.

Writing – original draft: IS, OC

Writing – review and editing: IS, CB, FC, AA, AM, OC

Funding Acquisition: AM, OC

Administrative support: IS, AM, OC

Abstract

Moving events on the skin can be perceived through vision and touch. How does the brain create a unified multisensory representation of motion directions initially acquired in different coordinate systems? We show that the middle occipito-temporal region (hMT+/V5), along with a fronto-parietal network, encodes visual and tactile directions using a common external frame of reference independent of body posture. We characterized brain activity using fMRI in participants exposed to directional visual and tactile motion stimuli across different hand postures. We demonstrate that individually and functionally defined hMT+/V5 shows univariate preference for both visual and tactile motion and encodes motion directions in distributed activity patterns. Unlike somatosensory regions, information about tactile directions was enhanced in right hMT+/V5 when mapped using an external as compared to a somatotopic frame of reference. Crossmodal decoding showed that tactile directions defined using an externally centered coordinate system, but not a somatotopic one, align with the representation of visual directions in rhMT+/V5 (both MT and MST). A whole brain searchlight group analysis confirmed these individually defined regions-of-interest results and extended the presence of an aligned visuo-tactile code for directional motion in external space to the parietal and dorsal prefrontal cortex. Our findings reveal a brain network involving hMT+/V5 that encodes motion directions in vision and touch using a common external frame of reference.

Introduction

Accurately extracting the direction of moving events is arguably one of the most crucial perceptual abilities for the survival of most living organisms. Moving events can be perceived through different senses, like vision and touch. In vision, information is acquired using a retinotopic coordinate system while touch informs us about objects and events in contact with our skin and is therefore acquired using a somatotopic coordinate system. How does the brain co-register such multisensory information that come in widely different formats? For instance, seamlessly swapping a mosquito travelling on the arm requires that the brain aligns the representation of moving information across vision and touch. This is a non-trivial computational challenge since visual and tactile information are initially encoded in different reference frames (retinotopic vs somatotopic, respectively) and sensory organs (e.g. eyes and limbs) constantly move relative to the external world (Heed et al., 2015). To solve this problem, the mind and brain must engage in a reformatting process: signals from one modality could be remapped into the reference frame of the other modality, or both could be remapped into a common reference frame that abstract from the initial topographic mapping of each sense (Avillac et al., 2004, 2005). The observation of bidirectional behavioral crossmodal motion aftereffects - from vision to touch and conversely - suggests that motion processing relies on shared representations across vision and touch (Konkle et al., 2009). But where in the brain can these aligned motion representations be found?

In primates, aligned spatial information across the senses has been classically attributed to multisensory convergence zones (Meyer & Damasio, 2009) such as the parietal (Avillac et al., 2004; Duhamel et al., 1997, 1998) and frontal cortices (Bremmer et al., 2001; Rizzolatti et al., 1981). For instance, within the parietal cortex, neurons in the Ventral Intraparietal (VIP) area exhibit preference for both visual (Colby et al., 1993) and tactile motion signals (Duhamel et al., 1998; Summers et al., 2009) and single-unit recordings in VIP show partially aligned receptive fields (RFs) across the senses (Avillac et al., 2005). Beyond fronto-parietal regions, it has been shown that the middle temporal region hMT+/V5 in humans, a region causally supporting visual motion processing (Albright, 1984; Beckers & Zeki, 1995; Zeki et al., 1991; Zihl et al., 1983), also show motion selective response for sounds (Battal et al., 2019; Dormal et al., 2016a; Poirier et al., 2005) and touch (Blake et al., 2004; Hagen et al., 2002; Ricciardi et al., 2007); but see (Jiang et al., 2015)). A recent study showed that the distributed representation of motion directions in vision is partially aligned with those of auditory direction (Rezk et al., 2020). It has further been shown that hMT+/V5 also encodes tactile motion direction in distributed pattern of activity (van Kemenade et al., 2014) and is causally involved in tactile motion direction discrimination (Amemiya et al., 2017; Ricciardi et al., 2011). However, whether hMT+/V5 transform incoming moving signals across the senses into a unified frame of reference independent of body posture remains unknown. Previous studies showed that the response of hMT+/V5 to moving visual signals is modulated by gaze direction, suggesting a non-retinotopic (often called "spatiotopic") representation of visual motion signals, a format that could also be used to integrate motion signals across other senses (Burr & Morrone, 2011; Crespi et al., 2011; d'Avossa et al., 2007; Melcher & Morrone, 2003).

Here, we investigated whether the hMT+/V5, as well as fronto-parietal regions, represent visual and tactile motion directions using a common neural code that is independent of body

posture. In a first functional Magnetic Resonance Imaging (fMRI) experiment, we relied on independent visual and tactile motion localizers to individually and functionally define motion selective regions in both vision and touch. In a separate fMRI experiment, we presented directional motion in vision and touch while manipulating the perceived axis of tactile motion direction by changing the hand positions of the participants. Using multivariate pattern analyses (MVPA) in the functionally-defined individual regions of interest (fROIs) and whole brain searchlight analyses, we reveal aligned patterned neural response to directional visual and tactile motion signals that is independent of body posture.

Methods

Participants

Twenty healthy participants (11 females; mean age ± SD = 25.15 ± 3.51 years; age range = 19–33 years) were recruited for this study. All participants were right-handed, as determined using the Edinburgh Handedness Inventory (Oldfield, 1971) and had normal or corrected-to-normal vision. Two participants volunteered exclusively for the directional motion decoding experiments but did not participate in the localizer experiments. Consequently, the localizer experiments were conducted with only eighteen participants. All participants were naïve to the purpose of the study and reported no history of neurological or psychiatric disorders. The study protocol was approved by the Research Ethics Committee of Cliniques Universitaires Saint-Luc and Université Catholique de Louvain (UCLouvain). Written informed consent was obtained from all participants before the experiments, and they received monetary compensation for their participation. All the experiments were conducted over a minimum of two sessions, each lasting approximately 1 hour and 45 minutes.

Experimental Setup

The experiments were conducted using a 3-Tesla GE MR scanner equipped with a 48-channel head coil (Signa™ Premier, General Electric Company, USA; serial number: 000000210036MR03; software version: 28-LX-MR, release: RX28.0_R04_2020.b). Participants lay comfortably on the scanner bed, viewing a screen positioned behind the scanner. Throughout the experiment, they held a response button in their left hand. For the tactile motion localizer, participants kept their right hand open (palm up) besides their body to facilitate tactile stimulation. In the directional motion decoding experiments, participants were instructed to adopt one of the two hand positions depending on the experimental condition. In the hand-up (HU) position, their forearm was positioned perpendicular to the body plane with the palm facing outward, while in the hand-down (HD) position, the forearm was kept parallel to the body plane, with the palm also facing outward (Figure 1A).

Stimuli

Visual Stimuli

Visual stimuli (Figure 1A) were presented on a black screen with a frame rate of 60 Hz and a resolution of 1920 x 1200 pixels, measuring 70 cm in width and 43.75 cm in height. Participants viewed the screen from a distance of 170 cm through a mirror mounted on the MRI head coil. The stimuli consisted of 300 white random dot kinematograms (RDKs) displayed within an invisible circular aperture, which was centered around a white fixation cross and occupied the full height of the screen (15° of visual angle). The dots could either remain static or move in one of four translational directions: left, right, up, or down, as well as radially receding or approaching. Each dot measured 0.25° in size, had a limited lifetime of 200 ms (Bex et al., 2003), and moved at a speed of 15°/s. The origin of each dot was randomized on each trial.

Tactile Stimuli

Tactile stimuli (Figure 1A) were delivered manually using a custom-built, 30 cm wide MRI-compatible brush. The trained experimenter (author Iqra Shahzad), who was specifically trained to deliver tactile stimuli with consistent timing and frequency, brushed the right palm of the participants following computer-controlled auditory cues, which were delivered via MRI-compatible earphones (S14 insert earphones, SensiMetrics, USA; http://www.sens.com/). Each swipe lasted approximately 1s. Participants were instructed to keep their eyes closed throughout all tactile runs, and compliance was monitored by the experimenter.

Experiments

Visual Motion Localizer

One run of visual motion localizer (Figure 1B) was implemented to localize hMT+/V5 both at the group-level and in each participant individually (Huk et al., 2002; Rezk et al., 2020). The hMT+/V5 region, located in the medial temporal area responds preferentially to moving stimuli compared to static stimuli. Since the visual stimuli were presented at fixation in the center of the screen, the localizer defined the whole hMT+/V5 complex which includes both MT and MST (see below for a specific MT/MST localizer). Visual motion and static conditions were generated using white random dot kinematograms (RDK) on a black background. Each run lasted 4 minutes and 51 seconds, starting with an initial 5.25 seconds of a blank screen and ending with 14 seconds of blank screen. Within the run, there were 12 blocks of alternating motion and static conditions, with the starting block counterbalanced across participants. The blocks were separated by an inter-block interval (IBI) of 5 to 7 seconds, chosen randomly. Each block lasted 17.4 seconds and included 6 trials of 2.4 seconds each, separated by an inter-stimulus interval (ISI) of 0.5 seconds. In the motion blocks, the dots moved in one of four directions – left, right, up, and down. Within a motion block, a trial consisted of an axis of motion direction – horizontal (leftward movement of 1.2s followed by rightward movement of 1.2s) or vertical (upward movement of 1.2s followed by downward movement of 1.2s) axis. In the static blocks, each trial (2.4s) consisted of the sequential presentation of two static dots configurations, each lasting for 1.2s (following the cycle of motion direction change). Participants were asked to fixate on the central fixation cross. In the motion blocks, they were asked to detect a repeated direction within a trial, for example, leftward followed by a leftward motion stimulus. In the static blocks, they were asked to press when the dots did not change configuration in the two sequential presentations. The number of targets in each block varied between 0 and 2, randomly distributed and balanced across motion and static conditions.

MT/MST visual motion localizer

Using visual radial-motion stimulation, a separate localizer was implemented to divide the hMT+/V5 complex into subregions that may be identified as homologs to a pair of macaque motion-responsive visual areas: the middle temporal area (MT) and the medial superior temporal area (MST) (Huk et al., 2002). MT, thought to have smaller retinotopically organized receptive fields should not respond to peripheral ipsilateral stimulation. MST, known to have larger receptive fields, is assumed to respond to peripheral visual motion stimulation in both ipsilateral and contralateral visual hemifields (Huk et al., 2002). One run of MT/MST localizer

(~7min) (Figure 1B) consisted of 20 blocks of stimulation: 10 blocks presented radial motion in the left hemifield, and the following 10 blocks presented the radial motion in the right hemifield, while the fixation was maintained in the opposite side of the screen i.e., right and left respectively. The order of presentation of the motion stimuli in the left or right hemifield was counterbalanced across participants. Within a block, there were 6 trials, where each trial consisted of receding (0.6s) followed by approaching (0.6s) RDKs. The dots were restricted to a circular aperture of radius 7° visual angle, with its edge 10° from fixation.

Each run started with a blank screen for 5s and ended with a blank screen for 14s. The inter-block interval (IBI) was 10s including trials during which participants had to change the fixation from one side to the other. Participants were asked to fixate their eyes on the fixation cross and detect changes in its color (white to red). The number of targets (range: 0-2 in each block) were randomized and balanced across conditions.

Tactile Motion Localizer

A tactile motion localizer (Figure 1B) was implemented to identify regions that respond preferentially to tactile motion. Each participant performed two runs of the tactile motion localizer (10min 49s each). Each run started with a blank screen of 5s and ended with a 14s pause. It included 20 blocks of alternating motion and static conditions with the starting condition counterbalanced across participants. The blocks were separated with an inter-block interval (IBI) chosen randomly between 5-7 s. Each block (19.5s) included 6 trials of 2s each and an inter-stimulus interval (ISI) of 0.5s. A motion trial consisted of a brush swipe on the right palm from pinky-to-thumb (1s) followed by thumb-to-pinky (1s) representing one somatotopic axis of motion, or from finger-to-wrist (1s) followed by wrist-to-finger (1s) representing the other somatotopic axis of motion. In the static trials, the brush was touched on the right palm sequentially across two somatotopic orientations: thumb-pinky (1s) and finger-wrist (1s). Participants kept their eyes closed throughout the run. In the motion blocks, they were asked to detect a repeated direction within a trial, for example, pinky-to-thumb followed by a pinky-to-thumb motion. In the static block, the participants were asked to detect the trials where the brush was touched in the same orientation consecutively. The number of targets within a block varied between 0 and 2 with the position of the target in the blocks randomized and balanced across conditions.

Directional Motion Decoding Experiments

The directional motion experiments (Figure 1C) were conducted to characterize the pattern of neural activity underlying perception of visual and tactile motion directions across two hand positions – HU and HD using multivariate pattern analyses (MVPA). These experiments involved the presentation of directional motion stimuli across 30 runs, such that 10 runs were performed for each sensory modality and each hand position - i.e. visual, tactile HU, tactile HD. The order of the 3 types of runs was counterbalanced across participants. Note that the participants were allowed to rest their right hand in a comfortable position during the visual runs and the motion stimuli used in these experiments were identical to those used in the localizer tasks. Each run lasted 3 min 18s, beginning with a 5s blank screen ending with a 14 s blank screen. Within each run, two directional motion stimuli were presented four times each in a randomized order. Thus, there were six motion conditions across 30 runs (visual:

horizontal (Vh) and vertical (Vv); tactile: hand up pinky-thumb (HUpt) and finger-wrist (HUfw); tactile: hand down pinky-thumb (HDpt) and finger-wrist (HDfw)). Each block (17s) comprised 7 trials of a directional stimulus along one axis-of-motion (either pinky-thumb or finger-wrist axis for tactile runs; either horizontal or vertical axis for visual runs), with an ISI of 0.5 s and an IBI chosen randomly between 5 and 7s.

MRI acquisition

A whole-brain T1-weighted anatomical scan was acquired (3D-MPRAGE; 1.0 x 1.0 mm in-plane resolution; slice thickness 1mm; no gap; inversion time = 900 ms; repetition time (TR) = 2189,12 ms; echo time (TE) = 2.96 ms; flip angle (FA) = 8°; 156 slices; field of view (FOV) = 256 x 256 mm^2; matrix size= 256 X 256).

Functional data for the localizers was acquired with T2*-weighted scans acquired with Echo Planar and gradient recalled (EP/GR) imaging (2.6 x 2.6 mm in-plane resolution; slice thickness = 2.6mm; no gap; Multiband factor = 2; TR = 1750ms, TE = 30ms, 58 interleaved ascending slices; FA = 75°; FOV = 220 x 220 mm^2; matrix size= 84 X 84). The number of volumes acquired in the visual motion localizer, tactile motion localizer and MT/MST visual localizer were 167, 372 and 282 volumes respectively.

Functional data for the directional motion decoding experiments were acquired with a T2*-weighted scans acquired with Echo Planar and gradient recalled (EP/GR) imaging (2.3 x 2.3 mm in-plane resolution; slice thickness = 2.3mm; no gap; Multiband factor = 2; TR = 1750ms, TE = 35ms, 52 interleaved ascending slices; FA = 75°; FOV = 216 x 216 mm^2; matrix size= 94 X 94). A total of 117 volumes were collected for each tactile HU and HD runs, while 114 volumes were collected for each visual runs.

Behavioral data analyses

The performance of participants in all the different experiments were analyzed and reported as mean accuracy of detecting targets with standard error. Two-sample t-tests were computed to check if there were differences in detection performance between two conditions within an experiment.

fMRI Preprocessing

The structural and functional data were pre-processed with BidSpm (v2.2.0; https://github.com/cpp-lln-lab/bidspm; Gau et al. 2022) using Statistical Parametric Mapping (SPM12 - 7771; Wellcome Center for Neuroimaging, London, UK; https://www.fil.ion.ucl.ac.uk/spm; RRID:SCR_007037) and MATLAB R2020b on a macOS (macOS Monterey Version 12.6) computer. The preprocessing of the functional images was performed in the following order: slice timing correction with reference to the middle slice; realignment and unwarping; segmentation and skullstripping; coregistration of functional and anatomic data; normalization to a template in Montreal Neurologic Institute (MNI) space and smooothing with all default options implemented in BidSpm. Slice timing correction was performed taking the 29th (middle) slice as a reference (interpolation: sinc interpolation). Functional scans from each participant were realigned and unwarped using the mean image as a reference (SPM single pass; number of degrees of freedom: 6; cost function: least square)

(Friston et al., 1995). The anatomical image was bias field corrected, segmented and normalized to MNI space (target space: IXI549Space; target resolution: 1 mm; interpolation: 4th degree b-spline) using a unified segmentation. The tissue probability maps generated by the segmentation were used to skullstrip the bias corrected image removing any voxel with p(gray matter) + p(white matter) + p(CSF) > 0.75. The mean functional image obtained from realignement was co-registered to the bias corrected anatomical image (number of degrees of freedom: 6; cost function: normalized mutual information) (Friston et al., 1995). The transformation matrix from this coregistration was applied to all the functional images. The deformation field obtained from the segmentation was applied to all the functional images (target space: IXI549Space; target resolution: equal to that used at acquisition; interpolation: 4th degree b-spline). Preprocessed functional images spatially smoothed using a 3D gaussian kernel (FWHM of 6mm for the localizers and 2mm for the directional motion decoding experiments). This section of preprocessing fMRI data was automatically generated using bidspm (Gau et al., 2022) and octache (https://github.com/Remi-Gau/Octache).

Univariate Analyses

For both visual and tactile motion localizer, a general linear model (GLM) was fitted for every voxel with the motion and the static conditions as regressors of interest in each subject. Each regressor was convolved with SPM canonical hemodynamic response function (HRF). The 6 head motion parameters (3 translation and 3 rotation parameters) were included in the model as regressors of no interest. The contrast (motion > static) was computed for every subject individually to identify functional regions-of-interest (fROIs) responding preferentially to motion stimuli in vision and touch. In addition, these individual contrasts were further smoothed with a 6 mm FWHM kernel and entered a random effects model for a standard second-level group analysis. Group-level statistical significance was assessed either using family-wise error (FWE) correction across the whole brain at a significance level of $p < 0.05$ or using small volume correction (SVC) within small spherical volumes (10 mm radius) around functional ROI coordinates. (STable 1 and STable2). Regions were labelled using the Automated Anatomical Labelling 3 (AAL3) atlas (Rolls et al., 2020) available in SPM12.

Similar approach was adopted for the univariate analyses of MT/MST visual motion localizer. A GLM was fitted for every voxel with left-hemifield motion and right-hemifield motion conditions as regressors of interest in each subject. Each regressor was convolved with SPM canonical hemodynamic response function (HRF). The 6 head motion parameters (3 translation and 3 rotation parameters) were included in the model as regressors of no interest. The contrasts (left-hemifield motion > baseline and right-hemifield motion > baseline) were computed for every subject individually. The conjunction of these contrasts revealed the MST area in each individual.

Functional Regions of Interest (fROI) definition

The individually defined motion selective functional regions of interest (fROIs) were created following the Group-Constrained Subject-Specific (GSS) method, which algorithmically detects fROIs that are systematically activated across subjects. This method is similar to a random effects analysis, but is more tolerant of anatomical variability across subjects, adding sensitivity and selectivity to the results. The GSS method has been successfully used to define

fROIs preferential for various visual categories (Julian et al., 2012), language (Fedorenko et al., 2010) and visual and auditory motion (Battal et al., 2022; Dormal et al., 2016b; Dormal & Collignon, 2011; Rezk et al., 2020). The visual motion selective area, hMT+/V5 was identified from the visual motion localizer using the contrast motion > static. First, hMT+/V5 was identified bilaterally at the group-level as the cluster of voxels ($p<0.05$ FWE) in the middle-temporal gyrus. The group-level spherical fROI mask (radius 12mm) was drawn around the group-level peak coordinate in each participant. Within this group-constrained mask, individually identified peak of motion selectivity (motion > static) was identified and an individual spherical fROI masks was selected (radius 8mm; ~ 176 voxels).

Further, MT/MST visual motion localizer was used to identify and create fROI masks of the sub-divisions of the hMT+/V5: MT and MST. MST was defined as the part of hMT+/V5 that responds to ipsilateral and contralateral visual motion stimulation. Therefore, individually localized clusters of MST voxels were constrained by the individually localized clusters of hMT+/V5 and used as fROIs masks in further analyses. Individual MT masks were defined as the part of hMT+/V5 that prefers contralateral over ipsilateral motion and therefore excludes MST.

Similar approach was adopted to identify tactile motion selective areas. Group level analyses first revealed the presence of tactile motion selective response in the postcentral gyrus and middle temporal cortex. As in the visual motion localizer, a 12mm spherical fROI mask was drawn around the group-level peak coordinate to constrain individual subject activity. Ultimately, an 8mm-radius spherical fROI mask was drawn around the individually identified peak coordinates. Spherical masks of tactile motion selective areas in the middle temporal cortex were created in the same manner and were referred to as MTt (Middle Temporal tactile).

To foreshadow the univariate results, tactile motion selective areas overlapped with the visual motion selective hMT+/V5 in the middle temporal cortex, showing that a part of hMT+/V5 is engaged in tactile motion processing. Since the individually defined hMT+/V5 and MTt overlapped with each other (see STable 4 for dice coefficients), we reported hMT+/V5 results in the main findings while presenting MTt results as supplement (SFigure 2). The analyses in hMT+/V5 and MTt produced similar results (Figure 3 and SFigure 2), which was expected given the substantial overlap between these regions (STable 4).

Multivariate Pattern Analyses (MVPA)

Multivariate pattern analyses (MVPA) were carried out to investigate the representation of visual and tactile motion-directions across different hand postures in each subject. They were performed on the GLM output of directional motion decoding experiments. A GLM was fitted for each run and in each subject. Depending on the type of run, the regressors of interest were the two axis-of-motion stimuli (visual: horizontal (Vh) and vertical (Vv); tactile: hand up pinky-thumb (HUpt) and finger-wrist (HUfw); tactile: hand down pinky-thumb (HDpt) and finger-wrist (HDfw)) and the 6 head motion parameters were included as regressors of no interest. One beta map corresponding to each condition from each run was obtained. In total, we computed a total of 60 beta maps for each subject (10 for Vh, Vv, HUpt, HUfw, HDpt, HDfw).

To improve the SNR of each beta map used for decoding, the 10 beta maps within each experimental condition (eg. Vh) were randomly paired and averaged to generate 5 pseudorun-beta maps. Henceforth, the general procedure involved binary classification of the different experimental conditions using linear Support Vector Machine (SVM) (C parameter = 1) implemented in CoSMoMVPA (http://www.cosmomvpa.org/) (Oosterhof et al., 2016) and LIBSVM (http://www.csie.ntu.edu.tw/;cjlin/libsvm) (Chang & Lin, 2011) following a leave-one-run-out cross-validation scheme. Since there were 45 unique combinations of the pseudoruns, this procedure was repeated 45 times.

The binary decoding of different experimental conditions was performed within the fROI created from the localizer experiments. The meta feature selector was used to keep the most informative 100 features/voxels within a fROI. This feature selection process not only ensures a similar number of voxels within a given region across participants, but, more importantly, identifies and selects voxels that are carrying the most relevant information across categories of stimuli (Cox & Savoy, 2003; De Martino et al., 2008); therefore, minimizing the chance to include voxels that carry noises unrelated to our categories of stimuli. The classifier was trained on 4 pseudorun-betas and tested on 1 pseudorun-beta. This step was repeated 5 times (N-fold cross-validation) where in each fold the classifier was tested on a different run. The performance of the classifier was reported as the classification/decoding accuracy for each subject by averaging the decoding accuracies across all cross-validation folds. Finally, the mean decoding accuracy was reported across all the subjects with its standard error. Above chance (0.5 for binary classification) decoding accuracy would indicate presence of axes of motion information.

Statistical significance of the mean decoding accuracies within a fROI was assessed using non-parametric methods that combine permutations and sign flipping (Nichols et al., 2005; Winkler et al., 2016; Xu et al., 2023). First, the observed mean decoding accuracy was calculated across the subjects. Then, 10,000 iterations of a sign-flipping procedure were performed to generate a group-level null distribution. In each iteration, the decoding accuracy of each subject was randomly assigned a reverse sign, and the mean decoding accuracy was recalculated for the group. This gave us 10,000 mean decoding accuracies which formed the group-level null distribution. Statistical significance was then determined by comparing the observed mean decoding accuracy to the null distribution, with the p-value defined as the proportion of null distribution values greater than or equal to the observed mean. To account for multiple comparisons across fROIs, all p values were corrected using false discovery rate (FDR) correction (Benjamini & Hochberg, 1995).

Within-modality decoding

To test the presence of visual motion direction information in motion-selective areas, binary classification of visual horizontal and visual vertical directions was implemented in the fROIs defined from the localizers– left somatosensory cortex, left and right hMT+/V5. Since hMT+/V5 (visually defined) and MTt (tactually defined) overlapped with each other, the decoding of visual motion information in MTt is presented in supplemental material. To further investigate the visual motion selectivity in the sub-divisions of hMT+/V5, classification was performed in the MST and MT fROIs masks separately.

Since tactile motion directions can be coded either in a somatotopic or in an external frame of reference depending on the hand positions, the four experimental conditions were rearranged to perform two different classifications in the motion-selective fROIs. The somatotopic frame of reference was decoded by classifying pinky-thumb direction versus finger-wrist direction pooled across the hand position. The external frame of reference was decoded by classifying horizontal (pinky-thumb in HU position pooled with finger-wrist in HD position) versus vertical (finger-wrist in HU position pooled with pinky-thumb in HD position) directions. To further study the recruitment of tactile frame of references in the different ROIs, the decoding accuracies were entered into a Linear Mixed Model (LMM) using the *lmer* function implemented in R (R Core Team, 2023). The frame of references (somatotopic, external) and the fROIs (lS1, left hMT+/V5, right hMT+/V5) were entered as fixed effects and subjects as a random effect. Finally, the tactile motion representation was investigated in the same manner in the MST, MT and the MTt fROIs separately.

Multi-Dimensional Scaling

Multi-Dimensional Scaling (MDS) was used to visualize the underlying spatial structure of the different motion directions across the sensory modalities in a single fROI. It allowed us to visualize the relative distance between the different pairs of motion directions across the sensory modalities. To do so, representational similarity analysis (RSA) (Kriegeskorte, 2008; Kriegeskorte et al., 2008) was first used to assess the underlying dissimilarities across the 6 different experimental conditions (visual horizontal, visual vertical, tactile pinky-thumb in somatotopic FoR, tactile finger-wrist in somatotopic FoR, tactile horizontal in external FoR, tactile vertical in external FoR). The dissimilarity matrix was created using the pairwise distances (metric "correlation distance" in CoSMoMvpa) for each subject and then averaged across subjects for a single fROI. The averaged dissimilarity matrices were visualized on an abstract cartesian map of 2-dimensions using DISTASIS (Abdi et al., 2005).

Cross-modal Decoding

To test the presence of shared axes of motion information across the senses, we performed crossmodal binary decoding of visual and tactile motion axes of motion within each fROIs – left somatosensory cortex, left hMT+/V5 and right hMT+/V5 and separately for MT, MST and MTt. Here, the classification was implemented using a similar cross-validation scheme as described above, except that the training set was chosen from one modality and the testing set from another modality. Also, note that prior to the cross-modal classification, the patterns of each motion direction corresponding to each modality were demeaned to equate their mean activity. Since the tactile motion directions could be decoded in two different frames of reference, crossmodal decoding was performed between (a) visual motion directions and tactile motion directions in a somatotopic frame of reference, and (b) visual motion directions and tactile motion directions in an external frame of reference. Note that the analytical procedure was the same for both (a) and (b) except the way the tactile stimulation was assigned to different classes. Finally, statistical inference of the mean decoding accuracies across both the direction of training and testing sets (train on vision, test on touch and vice versa) within each fROI are reported. The crossmodal decoding for the different directions of train and test sets are reported in supplemental material (SFigure 1).

Searchlight Analyses

In addition to the fROI-based MVPA, a whole-brain searchlight decoding method (Kriegeskorte et al., 2006) was implemented (as in (Rezk et al., 2020)) to identify regions representing visual and tactile motion information outside of our fROIs that we inferred from the visual and tactile motion localizers. To do so, a sphere (defined with a radius of 3 voxels) was moved across the brain volume, where the decoding accuracy of the features within the sphere is attributed to the center of the sphere. This method provides a whole-brain map of decoding accuracies for each voxel in each subject. The individual accuracy maps were smoothed with 8 mm FWHM smoothing kernel and entered in a second-level group analysis. Group-level maps were corrected using a small-volume correction (SVC) of 10-mm radius at the location of the group-level peak coordinates identified independently from the localizers (left hMT+/V5: -47, -70, 5 mm; right hMT+/V5: 47, -65, 3 mm). Since we did not obtain parietal areas as motion selective in group-level univariate analyses, we corrected the group-level searchlight maps at the location of tactile motion selective left and right parietal area (MNI coordinates left parietal area: -30, -53, 49 mm; right parietal area: 41, -55, 54 mm) identified from another study investigating tactile motion selectivity (Summers et al., 2009).

Results

Behavioral Responses

The behavioral performance of each participant was assessed in all experiments, measuring their ability to detect targets in each condition. STable 1 presents the mean accuracy in each task. Participants performed consistently well across all conditions, with no significant differences between motion and static conditions in the localizer experiments or between conditions (Vh and Vv; HUpt and HUfw; HDpt and HDfw) in the main decoding experiments (Wilcoxon signed rank test; all $p > 0.05$). This lack of difference in behavioral performance between conditions suggests that the observed motion selectivity in the localizers and the decoding results in the directional motion decoding experiments cannot be attributed to differences in performance or attention.

Visual Motion Localizer

STable 1 lists the regions showing preferential responses to visual motion at a threshold p=0.05 FWE corrected which are illustrated on Figure 2A. We found clusters of voxels in the left and right middle temporal gyrus (hMT+/V5) extending bilaterally to lingual gyrus (V1) and left V3a. The hMT+/V5 clusters were observed at the intersection of the ascending limb of inferior temporal sulcus and lateral occipital sulcus (Dumoulin, 2000). We did not observe regions such as VIP and LIP in the parietal cortex to be visual motion selective using our localizer approach which is also consistent with previous studies (Battal et al., 2022; Dormal et al., 2016b; Rezk et al., 2020; Zeki et al., 1991).

Tactile Motion Localizer

Similar approach was adopted to identify tactile motion selective areas from the whole brain univariate analyses and computation of the contrast tactile motion > tactile static (Figure 2A, STable 2). Consistent with previous studies (Ricciardi et al., 2007; Summers et al., 2009; van Kemenade et al., 2014), we observed preferential response to tactile motion in the left post central gyrus (left primary somatosensory cortex), bilateral rolandic operculum (secondary somatosensory cortex) and in the middle temporal gyrus. An overlay of the group-level contrasts (motion > static) revealed an overlap between the visual and tactile motion selective regions (Figure 2A). More precisely, 32.21% of voxels of visually defined left hMT+/V5 and 42.55% of voxels in right hMT+/V5 showed tactile motion selectivity. Similar to the visual motion localizer, we did not observe regions in the parietal cortex to be tactile motion selective.

To further investigate tactile motion selectivity within the individually localized bilateral hMT+/V5, we compared the beta parameters for tactile motion and static conditions within each individual's hMT+/V5 fROI (Figure 2B). One-tailed paired t-tests revealed that responses to tactile motion conditions were significantly higher than the static conditions in both fROIs (left hMT+/V5 ($t(17) = 1.99$, $p = 0.03$, $d = 0.24$) and right hMT+/V5 ($t(17) = 2.15$, $p = 0.02$, $d = 0.17$). The fROI left primary somatosensory cortex being tactile motion selective did not show visual motion selectivity ($t(17) = 0.47$, $p = 0.32$, $d = 0.09$).

MT/MST Localizer

Subregions of hMT+/V5, which are presumed homologs to the macaque middle temporal (MT) area and the medial superior temporal (MST) area, were identified in each individual (Huk et al., 2002). In each subject, we computed the conjunction (AND) (Nichols et al., 2005) of the contrasts left-hemifield motion > 0 and right-hemifield motion > 0 at a threshold of $p = 0.001$ uncorrected or $p = 0.05$ FWE corrected, and constrained the activity to the individually localized clusters of hMT+/V5 (from the visual motion localizer) to identify MST area. STable 3 shows the number of voxels in the identified clusters. Following this, MT voxels were defined as part of individually localized clusters of hMT+/V5 which do not belong to MST. We were able to reliably localize these regions in 14 out of the 18 tested participants. Figure 5A shows the identified clusters of MST and MT in one exemplar subject.

To investigate tactile motion selectivity within the individually localized MST and MT, tactile motion and static mean beta parameters extracted from the univariate analyses of tactile motion localizer were compared within each individual's MST and MT mask (Figure 5A). One-tailed paired t-tests (*p*-values subjected to Bonferroni correction for multiple comparisons) were performed to compare the motion and static conditions within each fROI. Beta parameters for motion conditions were significantly higher than the static conditions in all the fROIs (left MST ($t(13) = 3.37$, $p = 0.005$, $d = 0.39$), left MT ($t(13) = 3.13$, $p = 0.005$, $d = 0.18$), right MST ($t(13) = 4.76$, $p = 0.000$, $d = 0.37$), right MT ($t(13) = 3.49$, $p = 0.005$, $d = 0.25$)).

fROI-based MVPA

Functional Regions of Interest (fROIs)

Whole-brain univariate analyses for independent visual and tactile motion localizers (contrast motion>static) were performed to acquire the group-level coordinates of bilateral hMT+/V5 and left S1, selective to visual and tactile motion, respectively. The MNI group coordinates: left S1 [-44, -2, 60 mm]; left hMT+/V5: [-42, -65, 4 mm]; right hMT+/V5: [48, -63, 1 mm] were first used to create group-level spherical fROI masks of radius 12mm. Following this, individual peak coordinates, constrained by the group-level fROI masks were identified to create spherical fROI masks of radius 8mm. The MNI coordinates of these individual spherical fROI masks are shown in STable 5.

Since we observed preferential response to tactile motion from the tactile motion localizer in the hMT+/V5 region (for overlap, see Figure 2A), we performed separate MVPA in hMT+/V5 (defined visually) and MTt (defined tactually). Since the individually defined hMT+/V5 and MTt overlapped with each other (for dice coefficients see STable 7), results in hMT+/V5 are presented in the main manuscript and in MTt in supplemental; both fROIs yield similar results.

Foreshadowing our MVPA results, we observed significant crossmodal decoding only in the right hMT+/V5 (Figure 3C). Therefore, we performed MVPA in the individually identified clusters of MST and MT to further investigate the visual and tactile motion representations across different frames of reference solely in the right hemisphere. However, due to the variability in the size of the fROIs masks across participants (as shown in STable 1), we chose a subset of 8 subjects which had at least 30 voxels for MVPA. This allowed us to keep the same number of features/voxels for MVPA across regions and subjects.

Within-modality decoding

When decoding visual motion axes of motion (vertical versus horizontal), we obtained above-chance (0.5) decoding accuracies in both left (p<0.05; FDR-corrected) and right hMT+/V5 (p<0.05; FDR-corrected), but not the left S1 (p>0.05; FDR-corrected) (Figure 3A). A separate analysis in MTt (p<0.05) (Figure 5A) also revealed significant presence of visual motion information. MT and MST (Figure 5B) also suggest the presence of visual motion information.

To determine whether the tactile motion directions are presented within a somatotopic frame of reference or an externally-defined frame of reference, we performed decoding of tactile motion directions pooled across the hand postures. The somatotopic frame of reference was decoded within each fROI by classifying pinky-thumb vs finger-wrist tactile motion stimulation across the hand postures, and the external frame of reference was decoded by classifying externally-defined horizontal and vertical tactile directions across the hand postures (see Figure 1A for the design). Decoding accuracies obtained for each frame of reference (somatotopic, external) within the 3 fROIs (left S1, left hMT+/V5, right hMT+/V5) were tested against the chance level (0.5). The somatotopic encoding of tactile motion directions was reliably decoded in the left S1 and left hMT+/V5 (p < 0.05; FDR-corrected) and the decoding of external frame of reference was above chance in all the 3 fROIs- left S1, left hMT+/V5, right hMT+/V5 (p < 0.05; FDR-corrected) (Figure 3A). To further assess the recruitment of tactile frames of references within the fROIs, the decoding accuracies were entered into a Linear Mixed Model (LMM). The 2 frames of reference (somatotopic, external) and the 3 fROIs (left S1, left hMT+/V5, right hMT+/V5) were entered as fixed effects and subjects as a random effect. We observed a significant main effect of the fROIs (F (2,95) = 28.01, p = 0.00, ω^2 = 0.35), showing that the primary somatosensory area showed highest decoding accuracy owing to its primary function of processing tactile inputs. There was no significant main effect of the frames of reference (F (1,95) = 2.16, p = 0.144, ω^2 = 0.01). Crucially, there was a significant interaction of fROIs X FoR (F (2,95) = 11.25, p = 0.00, ω^2 = 0.17) suggesting that the relationship between decoding accuracy and frame of reference is dependent on the specific fROI. Post hoc paired t-tests (p-values subjected to FDR correction for multiple comparisons) were performed to compare the two frames of reference within each fROI. Decoding accuracies were significantly higher in the somatotopic frame of reference than the external frame of reference only in the left S1 (t (19) = 4.21, p = 0.0014, d = 1.13) supporting a dominant somatotopic representation of tactile motion directions in the primary somatosensory cortex. Although the decoding accuracy in the right hMT+/V5 seemed to be higher for external than the somatotopic frame of reference, likely explaining the significant interaction, the paired t-test revealed no significant differences in the right hMT+/V5 (t (19) = -1.37, p = 0.278, d = -0.43) and left hMT+/V5 (t (19) = -0.28, p = 0.78, d = -0.08) after FDR correction.

Since hMT+/V5 and MTt overlap, decoding of tactile motion frame of references in MTt showed a similar trend. The decoding of somatotopic frame of reference reliably above chance in left MTt (p = 0.029) and the decoding of external frame of reference was above chance in both, left MTt (p = 0.031) and right MTt (p = 0.015) (SFigure 2). Paired t-tests, however, revealed no significant differences between somatotopic and external coding of tactile motion direction (p < 0.05). Descriptively, the decoding accuracy appeared to be

higher for external than the somatotopic frame of reference in the right MTt as in the right hMT/V5.

Finally, the same analyses of decoding tactile motion directions in different frames of reference were performed separately in MST and MT fROIs. Similar to the decoding of touch in right hMT+/V5, individually defined right MT masks also showed seemingly higher decoding of tactile motion direction in external than somatotopic frame of reference (Figure 5B).

Multidimensional Scaling

To further investigate the representational layout in left S1 and right hMT+/V5, we used Multidimensional Scaling (MDS) to visualize the relative distances between the different motion direction conditions and project them on to an abstract 2-dimensional map (Figure 3B). First, MDS revealed a clear separation of the visual and tactile modalities within both fROIs. Secondly, we observed an interesting layout within the tactile modality. In the left S1, the somatotopically defined directions were farther apart than the externally defined directions supporting the reliable difference in decoding of the two tactile frames of reference. Conversely, in right hMT+/V5, externally defined directions were spaced further apart than the somatotopically defined directions, which also support the seemingly different decoding accuracies across the two frames of reference in right hMT+/V5.

Cross-Modal Decoding

To further investigate whether the motion information was shared across sensory modalities within our fROIs, we performed crossmodal decoding between visual and tactile motion directions defined (a) somatotopically and (b) externally (Figure 3C and SFigure 1). The crossmodal analysis between the visual and the tactile motion directions defined in a somatotopic frame of reference did not yield significant crossmodal decoding accuracies in any of the fROIs ($p > 0.05$). On the other hand, the same crossmodal analysis between the visual and tactile motion directions defined using an external frame of reference revealed significant cross-modal decoding accuracy selectively in the right hMT+/V5 ($p = 0.013$, FDR corrected). This shows that the motion information is shared across vision and touch in right hMT+/V5 only when the tactile motion directions are coded using an external frame of reference.

MTt also showed similar trend of results with significant crossmodal decoding of visual and tactile motion direction in external frame so reference present only in the right MTt ($p = 0.032$) (SFigure 2).

Interestingly, right MST and right MT also show the same trend of crossmodal decoding. The crossmodal decoding accuracies seemingly increase above the chance level in both right MST and right MT when the tactile motion directions are expressed in external frame of reference (Figure 5C).

Searchlight Decoding Analysis

To explore the larger network of regions showing motion-direction specificity across the sensory modalities and the different frames of reference beyond our fROIs, we implemented a whole-brain searchlight decoding analysis. Since we did not observe parietal and frontal areas as motion selective from our visual and tactile motion localizers (Figure1A), the searchlight method allowed us to also investigate the role of these regions. We performed the within-modal and cross-modal decoding and tested the statistical significance using Small Volume Correction (SVC) within a sphere of radius 10 mm. SVC (Table 3) was performed at the location of the left and right hMT+/V5 identified independently from the visual motion localizer (left hMT+/V5: -47, -70, 5 mm; right hMT+/V5: 47, -65, 3 mm) and on coordinates in the parietal regions obtained from a previous study that assessed the tactile motion selectivity (Summers et al., 2009) (Talairach coordinates left Intraparietal Area: -30,-50,45 and right Intraparietal Area: 42, -51, 49 converted to MNI coordinates left Intraparietal Area: -30,-53,49 mm and right Intraparietal Area: 41, -55, 54 mm, using Bioimage Suite Web : (www.bioimagesuite.org) (Lacadie et al., 2008)). Additionally, coordinates within the frontal cortex were obtained from previous studies on the external representation of touch (Crollen et al., 2017; Lloyd et al., 2003) were also tested for statistical significance using SVC in searchlight crossmodal decoding.

Group-level searchlight decoding of visual motion directions (horizontal versus vertical; Figure 4B) revealed bilateral hMT+/V5 (peak coordinate at left: -41.6, -72.9, 5.9 mm and right 43.5, -68.3, -1 mm) and a network of clusters in the primary visual cortex (V1) (left Cuneus: -14, -75, 29 mm; right Cuneus: 16, -82, 27 mm) extending through the superior occipital gyrus to superior parietal lobule (left superior parietal gyrus : -28, -50, 50 ; right superior parietal gyrus: 27, -55, 59 mm) and some clusters in the frontal lobe (left middle frontal gyrus: -28, -4, 52 mm; right middle frontal gyrus: 34, -2, 52 mm).

Searchlight decoding was also performed for tactile motion directions represented in both somatotopic (Figure 4A) and external frame (Figure 4C) of reference. Decoding of tactile somatotopic frame of reference (Figure 4A) show clusters in the left (peak coordinate: -44, -71, 8.2 mm) and right middle temporal gyrus (peak coordinate: 46, -52, -3.3 mm) with significant information about tactile somatotopic frame of reference in this area. We also observed an extensive network of the primary (left postcentral gyrus) and secondary somatosensory (Rolandic Operculum and Insula) areas with the parietal areas (superior parietal gyrus), the motor areas (precentral gyrus; supplementary motor area) and frontal lobe (middle superior frontal gyrus; superior frontal gyrus). Decoding of tactile external frame of reference (Figure 4C) revealed clusters bilaterally in the middle temporal area (middle temporal gyrus left: -48, -61, 15 mm and right: 44, -66, 1 mm); a network of parietal areas (left superior parietal gyrus), primary (left post central gyrus) and secondary (left rolandic operculum, left supramarginal gyrus) somatosensory areas, motor areas (left supplementary motor area, left precentral gyrus) and frontal areas (medial and superior frontal gyrus).

We finally performed crossmodal searchlight decoding between visual and tactile directions in both somatotopic and external frame of reference at the whole brain level. Crossmodal decoding between visual and tactile directions in somatotopic frame of reference (Figure 4D), did not reveal any significant clusters. On the other hand, crossmodal decoding between visual and tactile motion directions defined in the external reference frame (Figure 4E) revealed a distinct network involving the middle temporal gyrus (48, -59, 8 mm), right superior

frontal gyrus (25, -2, 52 mm) and right superior parietal gyrus (18, -66, 52 mm). The cluster in the middle temporal area closely overlapped with the hMT+/V5 identified from the visual motion localizer (dice coefficient = 0.9091). The cluster in the frontal cortex encompasses the frontal eye field (FEF) area (Vernet et al., 2014) and the dorsolateral prefrontal cortex (Lloyd et al., 2003). The cluster in the posterior parietal cortex includes LIPv, LIPd, MIP and VIP verified using the Glasser atlas (Glasser et al., 2016).

Discussion

We investigated where in the brain can we find aligned representation of visual and tactile motion directions using a common neural code that is independent of body posture. Using univariate analysis, we first confirm that hMT+/V5 – a region traditionally considered as uniquely visual (Jiang et al., 2015), is also involved in preferentially processing tactile motion over static information (Blake et al., 2004; Hagen et al., 2002; Ricciardi et al., 2007). We then reveal that directional tactile motion, like in vision, is encoded in distributed patterns of activity in hMT+/V5. By manipulating the hand posture, we see that the right hMT+/V5 encodes tactile motion directions using preferentially an external frame of reference, which is shared by both vision and touch. Notably, the representation of touch and vision aligns only when tactile motion directions are encoded in an external reference frame. Finally, our results reveal that hMT+/V5 operates as part of a network involving frontal-parietal regions, which together serve as a distributed neural substrate aligning multisensory motion direction signals.

Using independent visual and tactile motion localizers, we identified regions that preferentially respond to visual and tactile motion directions at the group (Figure 2A) and individual level (Figure 2C). A significant part of hMT+/V5 exhibited preferential response to both visual and tactile motion directions (43% of rhMT+/V5 voxels), whereas the somatosensory regions responded exclusively to tactile motion. Previous studies have debated whether such motion selective responses to non-visual input were limited to MST but not MT (Beauchamp et al., 2007) or suggested that previous observation of tactile motion signal in hMT+/V5 is due to group averaging (Jiang et al., 2015). Our findings provide unequivocal evidence that parts of hMT+/V5 (Figure 2B), including both MT and MST subdivisions (Figure 5A), preferentially responds to both visual and tactile motion over static stimuli. These preferential activations for tactile motion in regions classically considered purely visual were not a byproduct of spurious group averaging as the tactile motion activity was extracted from individually defined fROIs using independent localizers.

Using MVPA, we investigated the representations of axes of visual and tactile motion within our fROIs and across the different hand postures (Figure 3A). As expected, we found that the visual axes of motion directions can be decoded in bilateral hMT+/V5. In primates, a key organizational feature of this region is that the cortical columns tuned to a specific motion direction are adjacent to those tuned to its 180-degree opposite, implementing an axis-of-motion hyper-columnar organization (Albright, 1984). Such organization likely underlies the ability to decode axes of motion from the neural activity recorded with fMRI in humans (Bartels et al., 2008; Kamitani & Tong, 2006; Schneider et al., 2019; Zimmermann et al., 2011).

We further examined whether the tactile motion directions can be decoded in hMT+/V5 and if so whether it is represented using a somatotopic and/or external frame of reference. The external representation of tactile motion entails a transformation of tactile motion inputs from skin-based coordinates to external space by taking hand postures into account (Badde & Heed, 2016; Heed et al., 2015, 2016). It implies that the tactile directions have been abstracted from the skin surface: a given direction is coded relative to external space, no matter on which skin location it was originally received. In our study, we do not determine the exact anchor of the external reference frame: changes in hand posture altered the

perceived axis of tactile motion on the skin, but the potential anchors, such as the eyes, head and trunk, remained unchanged. Thus, in our study, we use external frame of reference to refer to a representation that is non-somatotopic.

The left S1 shows significant representation of tactile motion directions in both frames of reference, though the representation was stronger in somatotopic compared to the external reference frame. This dominant somatotopic representation of tactile motion in the S1 aligns with its crucial role in processing primary tactile inputs. Previous studies in macaques have demonstrated that somatosensory neurons, particularly in areas 1, 2, and 3b, are strongly tuned to specific tactile motion directions (Pei et al., 2011; Pei & Bensmaia, 2014). Recent evidence suggests that area 3b neurons can integrate both cutaneous and proprioceptive information from the hand (Trzcinski et al., 2023), which may account for the expression of external reference frame in this region, albeit to a lesser extent than the somatotopic representation. The left hMT+/V5 demonstrates significant representation of tactile motion in both the somatotopic and external reference frames, with no statistically significant differences between them. In contrast, the right hMT+/V5 does not show a significant somatotopic representation of tactile motion but does exhibit a significant representation in external space, again with no statistically significant difference between the two frames of reference. Multidimensional scaling (Figure 3B) further illustrates these findings, revealing that tactile motion directions defined within the external reference frame are represented as more distinct in the right hMT+/V5 when compared to somatotopic representation of directional motion. This contrasts sharply with the left S1 (and even left hMT+/V5), where somatotopically defined tactile motion directions are represented as more widely separated. These results indicate that the right hMT+/V5 relies more on a non-somatotopic, external frame of reference for encoding tactile motion directions.

Importantly, we observed significant crossmodal decoding between visual and tactile axes of motion (Figure 3C) in the right hMT+/V5 when the tactile motion directions are expressed in an external frame of reference. This suggests that the alignment of visual and tactile spatial maps in hMT+/V5 occurs in a partially common reference frame when somatotopic coordinates have been integrated with the hand posture information. The spatial selectivity of hMT+/V5 seems to be anchored to an external, rather than a somatotopic (our results) or retinotopic (Burr & Morrone, 2011; Crespi et al., 2011; d'Avossa et al., 2007) reference frame which may be instrumental in constructing a stable representation of the dynamic world for action, despite continuous eye and hand movements. Previous fMRI studies have also highlighted the role of hMT+/V5 in multisensory processing across visual and auditory modalities (Alink et al., 2008; Battal et al., 2022; Gurtubay-Antolin et al., 2021; Lewis & Noppeney, 2010; Rezk et al., 2020; Sadaghiani et al., 2009; Van der Stoep & Alais, 2020). Our findings extend this role by demonstrating shared motion information across vision and touch in an external reference frame, further emphasizing hMT+/V5's crucial role in providing a common representational format of motion direction across the senses. The fROI-based MVPA was also performed in a subset of the individually localized right MST and right MT (Figure 5B and 5C) to attribute the representations of visual and tactile motion directions to the subdivisions of right hMT+/V5. We observed that tactile motion selectivity in an external frame of reference seem to be present in both MST and MT areas. The presence of shared

crossmodal motion information in both right MST and right MT suggest that both the subdivisions are playing a role in the alignment.

To identify regions outside our a priori fROI hypothesis, we finally performed group-level searchlight decoding analyses (Figure 4). The within-modality searchlight confirmed that the primary sensory cortices contain distinct representations of their respective sensory modalities. Searchlight decoding of visual motion directions (Figure 4B) revealed the primary visual cortex (V1), hMT+/V5 and dorsal stream regions. Likewise, tactile searchlight decoding in both somatotopic (Figure 4A), and external (Figure 4C) reference frame revealed an extensive network of the somatosensory (S1 and S2) cortices along with the hMT+/V5. Crossmodal searchlight decoding between vision and touch (Figure 4C and 4D) confirmed our fROI findings by demonstrating that the right hMT+/V5 align visual and tactile motion directions using an externally defined frame of reference. Alignment between visual motion and tactile motion coded using an external reference frame revealed additional frontal and parietal regions, such as the LIP and VIP in the posterior parietal cortex (PPC) and the FEF in the frontal cortex. The PPC and the frontal areas have long been known to be involved in the automatic remapping of touch in the external space (Azañón & Soto-Faraco, 2008a; Bruns & Röder, 2010; Crollen et al., 2017; Soto-Faraco & Azañón, 2013), as well as in the integration of multisensory spatial information (Andersen et al., 1997; Azañón & Soto-Faraco, 2008b; Lloyd et al., 2003; Serino et al., 2011). Our results therefore demonstrate that hMT+/V5 along with a frontal-parietal network play a key role in the alignment of motion directions across the senses.

It is unclear if the alignment across the senses occurs in a common abstract frame of reference or whether it is remapped to an anchor of a single modality. Previous studies have suggested that the automatic external mapping of tactile coordinates use visual coordinates (Azañón & Soto-Faraco, 2007). However, it is also argued that the remapping of touch in fronto-parietal network is not completely visual but also derived from motor planning and orienting actions (Heed & Röder, 2012). The frontal-parietal-hMT+/V5 network could also flexibly use different reference frames depending on task demand. For example, hMT+/V5 is tuned to a non-retinotopic reference frame during tasks with lower attentional demands but shifts to a retinotopic reference frame when attention is directed to the fovea during continuous and demanding visual discrimination tasks (Burr & Morrone, 2011; Crespi et al., 2011; d'Avossa et al., 2007; Gardner et al., 2008). Posterior parietal cortex flexibly updates its selectivity from representing sensory information during target localization to representing the movement goal during motor planning (Klautke et al., 2022). Our study therefore opens the door to further exploration on how different regions of the frontal-parietal-hMT+/V5 network flexibly cooperate to align crossmodal frame of references based on task demands (Rohe et al., 2019; Rohe & Noppeney, 2015, 2016).

It can be argued that imagining visual motion can evoke a selective response in hMT+/V5, and that therefore the direction of tactile motion can be decoded from visual imagery. Early visual areas like V1 engages in visual imagery (Kosslyn et al., 1993), and the direction of imagined visual motion can be decoded from V1 (Emmerling et al., 2016). However, our crossmodal decoding of visual and tactile motion directions did not reveal aligned representations in V1 (SFigure 3). We therefore conjecture that if the aligned motion

representation in hMT+/V5 was a byproduct of visual imagery, similar effects should have been observed in V1.

In conclusion, our study demonstrates that the right hMT+/V5, traditionally known for supporting visual motion signals, also represents tactile motion directions using an external frame of reference which aligns with the representation of visual motion directions. hMT+/V5 is part of the fronto-parietal network which contains shared representation of multimodal motion signals that may support efficient and optimal perception of the external dynamic world. Our results open new avenue for research on how biological, but also non-biological, neural networks implement coordinate transformation across the senses to guide coordinated action to moving events in the external world.

References

Abdi, H., O'Toole, A. J., Valentin, D., & Edelman, B. (2005). DISTATIS: The Analysis of Multiple Distance Matrices. *2005 IEEE Computer Society Conference on Computer Vision and Pattern Recognition (CVPR'05) - Workshops*, *3*, 42–42. https://doi.org/10.1109/CVPR.2005.445

Albright, T. D. (1984). Direction and orientation selectivity of neurons in visual area MT of the macaque. *Journal of Neurophysiology*, *52*(6), 1106–1130. https://doi.org/10.1152/jn.1984.52.6.1106

Alink, A., Singer, W., & Muckli, L. (2008). Capture of Auditory Motion by Vision Is Represented by an Activation Shift from Auditory to Visual Motion Cortex. *The Journal of Neuroscience*, *28*(11), 2690–2697. https://doi.org/10.1523/JNEUROSCI.2980-07.2008

Amemiya, T., Beck, B., Walsh, V., Gomi, H., & Haggard, P. (2017). Visual area V5/hMT+ contributes to perception of tactile motion direction: A TMS study. *Scientific Reports*, *7*(1), 40937. https://doi.org/10.1038/srep40937

Andersen, R. A., Snyder, L. H., Bradley, D. C., & Xing, J. (1997). MULTIMODAL REPRESENTATION OF SPACE IN THE POSTERIOR PARIETAL CORTEX AND ITS USE IN PLANNING MOVEMENTS. *Annual Review of Neuroscience*, *20*(1), 303–330. https://doi.org/10.1146/annurev.neuro.20.1.303

Avillac, M., Denève, S., Olivier, E., Pouget, A., & Duhamel, J.-R. (2005). Reference frames for representing visual and tactile locations in parietal cortex. *Nature Neuroscience*, *8*(7), 941–949. https://doi.org/10.1038/nn1480

Avillac, M., Olivier, E., Den□ve, S., Ben Hamed, S., & Duhamel, J.-R. (2004). Multisensory integration in multiple reference frames in the posterior parietal cortex. *Cognitive Processing*, *5*(3). https://doi.org/10.1007/s10339-004-0021-3

Azañón, E., & Soto-Faraco, S. (2007). Alleviating the 'crossed-hands' deficit by seeing uncrossed rubber hands. *Experimental Brain Research*, *182*(4), 537–548. https://doi.org/10.1007/s00221-007-1011-3

Azañón, E., & Soto-Faraco, S. (2008a). Changing Reference Frames during the Encoding of Tactile Events. *Current Biology*, *18*(14), 1044–1049. https://doi.org/10.1016/j.cub.2008.06.045

Azañón, E., & Soto-Faraco, S. (2008b). Changing Reference Frames during the Encoding of Tactile Events. *Current Biology*, *18*(14), 1044–1049. https://doi.org/10.1016/j.cub.2008.06.045

Badde, S., & Heed, T. (2016). Towards explaining spatial touch perception: Weighted integration of multiple location codes. *Cognitive Neuropsychology*, *33*(1–2), 26–47. https://doi.org/10.1080/02643294.2016.1168791

Bartels, A., Logothetis, N. K., & Moutoussis, K. (2008). fMRI and its interpretations: An illustration on directional selectivity in area V5/MT. *Trends in Neurosciences*, *31*(9), 444–453. https://doi.org/10.1016/j.tins.2008.06.004

Battal, C., Gurtubay-Antolin, A., Rezk, M., Mattioni, S., Bertonati, G., Occelli, V., Bottini, R., Targher, S., Maffei, C., Jovicich, J., & Collignon, O. (2022). Structural and Functional Network-Level Reorganization in the Coding of Auditory Motion Directions and Sound Source Locations in the Absence of Vision. *The Journal of Neuroscience*, *42*(23), 4652–4668. https://doi.org/10.1523/JNEUROSCI.1554-21.2022

Battal, C., Rezk, M., Mattioni, S., Vadlamudi, J., & Collignon, O. (2019). Representation of Auditory Motion Directions and Sound Source Locations in the Human Planum Temporale. *The Journal of Neuroscience*, *39*(12), 2208–2220. https://doi.org/10.1523/JNEUROSCI.2289-18.2018

Beauchamp, M. S., Yasar, N. E., Kishan, N., & Ro, T. (2007). Human MST But Not MT Responds to Tactile Stimulation. *Journal of Neuroscience*, *27*(31), 8261–8267. https://doi.org/10.1523/JNEUROSCI.0754-07.2007

Beckers, G., & Zeki, S. (n.d.). *The consequences of inactivating areas VI and V5 on visual motion perception*.

Benjamini, Y., & Hochberg, Y. (1995). Controlling the False Discovery Rate: A Practical and Powerful Approach to Multiple Testing. *Journal of the Royal Statistical Society Series B: Statistical Methodology*, *57*(1), 289–300. https://doi.org/10.1111/j.2517-6161.1995.tb02031.x

Bex, P. J., Dakin, S. C., & Simmers, A. J. (2003). The shape and size of crowding for moving targets. *Vision Research*, *43*(27), 2895–2904. https://doi.org/10.1016/S0042-6989(03)00460-7

Blake, R., Sobel, K. V., & James, T. W. (2004). Neural Synergy Between Kinetic Vision and Touch. *Psychological Science*, *15*(6), 397–402. https://doi.org/10.1111/j.0956-7976.2004.00691.x

Bremmer, F., Schlack, A., Duhamel, J.-R., Graf, W., & Fink, G. R. (2001). Space Coding in Primate Posterior Parietal Cortex. *NeuroImage*, *14*(1), S46–S51. https://doi.org/10.1006/nimg.2001.0817

Bruns, P., & Röder, B. (2010). Tactile capture of auditory localization: An event-related potential study: Tactile capture of auditory localization. *European Journal of Neuroscience*, *31*(10), 1844–1857. https://doi.org/10.1111/j.1460-9568.2010.07232.x

Burr, D. C., & Morrone, M. C. (2011). Spatiotopic coding and remapping in humans. *Philosophical Transactions of the Royal Society B: Biological Sciences*, *366*(1564), 504–515. https://doi.org/10.1098/rstb.2010.0244

Caruso, V. C., Pages, D. S., Sommer, M. A., & Groh, J. M. (2018). Beyond the labeled line: Variation in visual reference frames from intraparietal cortex to frontal eye fields and the superior colliculus. *Journal of Neurophysiology*, *119*(4), 1411–1421. https://doi.org/10.1152/jn.00584.2017

Caruso, V. C., Pages, D. S., Sommer, M. A., & Groh, J. M. (2021). Compensating for a shifting world: Evolving reference frames of visual and auditory signals across three multimodal brain areas. *Journal of Neurophysiology*, *126*(1), 82–94. https://doi.org/10.1152/jn.00385.2020

Chang, C.-C., & Lin, C.-J. (2011). LIBSVM: A library for support vector machines. *ACM Transactions on Intelligent Systems and Technology*, *2*(3), 1–27. https://doi.org/10.1145/1961189.1961199

Colby, C. L., Duhamel, J. R., & Goldberg, M. E. (1993). Ventral intraparietal area of the macaque: Anatomic location and visual response properties. *Journal of Neurophysiology*, *69*(3), 902–914. https://doi.org/10.1152/jn.1993.69.3.902

Cox, D. D., & Savoy, R. L. (2003). Functional magnetic resonance imaging (fMRI) "brain reading": Detecting and classifying distributed patterns of fMRI activity in human visual cortex. *NeuroImage*, *19*(2), 261–270. https://doi.org/10.1016/S1053-8119(03)00049-1

Crespi, S., Biagi, L., d'Avossa, G., Burr, D. C., Tosetti, M., & Morrone, M. C. (2011). Spatiotopic Coding of BOLD Signal in Human Visual Cortex Depends on Spatial Attention. *PLoS ONE*, *6*(7), e21661. https://doi.org/10.1371/journal.pone.0021661

Crollen, V., Albouy, G., Lepore, F., & Collignon, O. (2017). How visual experience impacts the internal and external spatial mapping of sensorimotor functions. *Scientific Reports*, *7*(1), 1022. https://doi.org/10.1038/s41598-017-01158-9

d'Avossa, G., Tosetti, M., Crespi, S., Biagi, L., Burr, D. C., & Morrone, M. C. (2007). Spatiotopic selectivity of BOLD responses to visual motion in human area MT. *Nature Neuroscience*, *10*(2), 249–255. https://doi.org/10.1038/nn1824

De Martino, F., Valente, G., Staeren, N., Ashburner, J., Goebel, R., & Formisano, E. (2008). Combining multivariate voxel selection and support vector machines for mapping and classification of fMRI spatial patterns. *NeuroImage*, *43*(1), 44–58. https://doi.org/10.1016/j.neuroimage.2008.06.037

Dormal, G., & Collignon, O. (2011). Functional selectivity in sensory-deprived cortices. *Journal of Neurophysiology*, *105*(6), 2627–2630. https://doi.org/10.1152/jn.00109.2011

Dormal, G., Rezk, M., Yakobov, E., Lepore, F., & Collignon, O. (2016a). Auditory motion in the sighted and blind: Early visual deprivation triggers a large-scale imbalance between auditory and "visual" brain regions. *NeuroImage*, *134*, 630–644. https://doi.org/10.1016/j.neuroimage.2016.04.027

Dormal, G., Rezk, M., Yakobov, E., Lepore, F., & Collignon, O. (2016b). Auditory motion in the sighted and blind: Early visual deprivation triggers a large-scale imbalance between auditory and "visual" brain regions. *NeuroImage*, *134*, 630–644. https://doi.org/10.1016/j.neuroimage.2016.04.027

Duhamel, J.-R., Bremmer, F., Ben Hamed, S., & Graf, W. (1997). Spatial invariance of visual receptive fields in parietal cortex neurons. *Nature*, *389*(6653), 845–848. https://doi.org/10.1038/39865

Duhamel, J.-R., Colby, C. L., & Goldberg, M. E. (1998). Ventral Intraparietal Area of the Macaque: Congruent Visual and Somatic Response Properties. *Journal of Neurophysiology*, *79*(1), 126–136. https://doi.org/10.1152/jn.1998.79.1.126

Dumoulin, S. O. (2000). A New Anatomical Landmark for Reliable Identification of Human Area V5/MT: A Quantitative Analysis of Sulcal Patterning. *Cerebral Cortex*, *10*(5), 454–463. https://doi.org/10.1093/cercor/10.5.454

Emmerling, T. C., Zimmermann, J., Sorger, B., Frost, M. A., & Goebel, R. (2016). Decoding the direction of imagined visual motion using 7 T ultra-high field fMRI. *NeuroImage*, *125*, 61–73. https://doi.org/10.1016/j.neuroimage.2015.10.022

Fedorenko, E., Hsieh, P.-J., Nieto-Castañón, A., Whitfield-Gabrieli, S., & Kanwisher, N. (2010). New Method for fMRI Investigations of Language: Defining ROIs Functionally in Individual Subjects. *Journal of Neurophysiology*, *104*(2), 1177–1194. https://doi.org/10.1152/jn.00032.2010

Gardner, J. L., Merriam, E. P., Movshon, J. A., & Heeger, D. J. (2008). Maps of Visual Space in Human Occipital Cortex Are Retinotopic, Not Spatiotopic. *The Journal of Neuroscience*, *28*(15), 3988–3999. https://doi.org/10.1523/JNEUROSCI.5476-07.2008

Gau, R., Barilari, M., Battal, C., Caron-Guyon, J., Cerpelloni, F., Falagiarda, F., MacLean, M., Mattioni, S., Rezk, M., Shahzad, I., Yang, Y., & Collignon, O. (2023). Bidspm: An spm-centric bids app for flexible statistical analysis. In Organization for Human Brain Mapping 2023.

Glasser, M. F., Coalson, T. S., Robinson, E. C., Hacker, C. D., Harwell, J., Yacoub, E., Ugurbil, K., Andersson, J., Beckmann, C. F., Jenkinson, M., Smith, S. M., & Van Essen, D. C. (2016). A multi-modal parcellation of human cerebral cortex. *Nature*, *536*(7615), 171–178. https://doi.org/10.1038/nature18933

Gurtubay-Antolin, A., Battal, C., Maffei, C., Rezk, M., Mattioni, S., Jovicich, J., & Collignon, O. (2021). Direct Structural Connections between Auditory and Visual

Motion-Selective Regions in Humans. *The Journal of Neuroscience*, *41*(11), 2393–2405. https://doi.org/10.1523/JNEUROSCI.1552-20.2021

Hagen, M. C., Franzén, O., McGlone, F., Essick, G., Dancer, C., & Pardo, J. V. (2002). Tactile motion activates the human middle temporal/V5 (MT/V5) complex: Tactile motion in hMT/V5. *European Journal of Neuroscience*, *16*(5), 957–964. https://doi.org/10.1046/j.1460-9568.2002.02139.x

Heed, T., Backhaus, J., Röder, B., & Badde, S. (2016). Disentangling the External Reference Frames Relevant to Tactile Localization. *PLOS ONE*, *11*(7), e0158829. https://doi.org/10.1371/journal.pone.0158829

Heed, T., Buchholz, V. N., Engel, A. K., & Röder, B. (2015). Tactile remapping: From coordinate transformation to integration in sensorimotor processing. *Trends in Cognitive Sciences*, *19*(5), 251–258. https://doi.org/10.1016/j.tics.2015.03.001

Heed, T., & Röder, B. (2012). The Body in a Multisensory World. In M. M. Murray (Eds.) et. al., *The Neural Bases of Multisensory Processes*. CRC Press/Taylor & Francis

Huk, A. C., Dougherty, R. F., & Heeger, D. J. (2002). Retinotopy and Functional Subdivision of Human Areas MT and MST. *The Journal of Neuroscience*, *22*(16), 7195–7205. https://doi.org/10.1523/JNEUROSCI.22-16-07195.2002

Jiang, F., Beauchamp, M. S., & Fine, I. (2015). Re-examining overlap between tactile and visual motion responses within hMT + and STS. *NeuroImage*, *119*, 187–196. https://doi.org/10.1016/j.neuroimage.2015.06.056

Julian, J. B., Fedorenko, E., Webster, J., & Kanwisher, N. (2012). An algorithmic method for functionally defining regions of interest in the ventral visual pathway. *NeuroImage*, *60*(4), 2357–2364. https://doi.org/10.1016/j.neuroimage.2012.02.055

Kamitani, Y., & Tong, F. (2006). Decoding Seen and Attended Motion Directions from Activity in the Human Visual Cortex. *Current Biology*, *16*(11), 1096–1102. https://doi.org/10.1016/j.cub.2006.04.003

Klautke, J., Foster, C., Medendorp, W. P., & Heed, T. (2022). *Dynamic spatial coding in parietal cortex mediates tactile-motor transformation* [Preprint]. Neuroscience. https://doi.org/10.1101/2022.11.12.516245

Konkle, T., Wang, Q., Hayward, V., & Moore, C. I. (2009). Motion Aftereffects Transfer between Touch and Vision. *Current Biology*, *19*(9), 745–750. https://doi.org/10.1016/j.cub.2009.03.035

Kosslyn, S. M., Alpert, N. M., Thompson, W. L., Maljkovic, V., Weise, S. B., Chabris, C. F., Hamilton, S. E., Rauch, S. L., & Buonanno, F. S. (1993). Visual Mental Imagery Activates Topographically Organized Visual Cortex: PET Investigations. *Journal of Cognitive Neuroscience*, *5*(3), 263–287. https://doi.org/10.1162/jocn.1993.5.3.263

Kriegeskorte, N. (2008). Representational similarity analysis – connecting the branches of systems neuroscience. *Frontiers in Systems Neuroscience*. https://doi.org/10.3389/neuro.06.004.2008

Kriegeskorte, N., Goebel, R., & Bandettini, P. (2006). Information-based functional brain mapping. *Proceedings of the National Academy of Sciences*, *103*(10), 3863–3868. https://doi.org/10.1073/pnas.0600244103

Kriegeskorte, N., Mur, M., Ruff, D. A., Kiani, R., Bodurka, J., Esteky, H., Tanaka, K., & Bandettini, P. A. (2008). Matching Categorical Object Representations in Inferior Temporal Cortex of Man and Monkey. *Neuron*, *60*(6), 1126–1141. https://doi.org/10.1016/j.neuron.2008.10.043

Lacadie, C. M., Fulbright, R. K., Rajeevan, N., Constable, R. T., & Papademetris, X. (2008). More accurate Talairach coordinates for neuroimaging using non-linear registration. *NeuroImage*, *42*(2), 717–725. https://doi.org/10.1016/j.neuroimage.2008.04.240

Lewis, R., & Noppeney, U. (2010). Audiovisual Synchrony Improves Motion Discrimination via Enhanced Connectivity between Early Visual and Auditory Areas. *The Journal of Neuroscience*, *30*(37), 12329–12339. https://doi.org/10.1523/JNEUROSCI.5745-09.2010

Lloyd, D. M., Shore, D. I., Spence, C., & Calvert, G. A. (2003). Multisensory representation of limb position in human premotor cortex. *Nature Neuroscience*, *6*(1), 17–18. https://doi.org/10.1038/nn991

Melcher, D., & Morrone, M. C. (2003). Spatiotopic temporal integration of visual motion across saccadic eye movements. *Nature Neuroscience*, *6*(8), 877–881. https://doi.org/10.1038/nn1098

Meyer, K., & Damasio, A. (2009). *Convergence and divergence in a neural architecture for recognition and memory*. *32*(7). https://doi.org/10.1016/j.tins.2009.04.002.

Nichols, T., Brett, M., Andersson, J., Wager, T., & Poline, J.-B. (2005). Valid conjunction inference with the minimum statistic. *NeuroImage*, *25*(3), 653–660. https://doi.org/10.1016/j.neuroimage.2004.12.005

Oldfield, R. C. (1971). The assessment and analysis of handedness: The Edinburgh inventory. *Neuropsychologia*, *9*(1), 97–113. https://doi.org/10.1016/0028-3932(71)90067-4

Oosterhof, N. N., Connolly, A. C., & Haxby, J. V. (2016). CoSMoMVPA: Multi-Modal Multivariate Pattern Analysis of Neuroimaging Data in Matlab/GNU Octave. *Frontiers in Neuroinformatics*, *10*. https://doi.org/10.3389/fninf.2016.00027

Pei, Y.-C., & Bensmaia, S. J. (2014). The neural basis of tactile motion perception. *Journal of Neurophysiology*, *112*(12), 3023–3032. https://doi.org/10.1152/jn.00391.2014

Pei, Y.-C., Hsiao, S. S., Craig, J. C., & Bensmaia, S. J. (2011). Neural Mechanisms of Tactile Motion Integration in Somatosensory Cortex. *Neuron*, *69*(3), 536–547. https://doi.org/10.1016/j.neuron.2010.12.033

Poirier, C., Collignon, O., DeVolder, A. G., Renier, L., Vanlierde, A., Tranduy, D., & Scheiber, C. (2005). Specific activation of the V5 brain area by auditory motion processing: An fMRI study. *Cognitive Brain Research*, *25*(3), 650–658. https://doi.org/10.1016/j.cogbrainres.2005.08.015

Pouget, A., Deneve, S., & Duhamel, J.-R. (2002). A computational perspective on the neural basis of multisensory spatial representations. *Nature Reviews Neuroscience*, *3*(9), 741–747. https://doi.org/10.1038/nrn914

Pouget, A., & Sejnowski, T. J. (1997). Spatial Transformations in the Parietal Cortex Using Basis Functions. *Journal of Cognitive Neuroscience*, *9*(2), 222–237. https://doi.org/10.1162/jocn.1997.9.2.222

Rezk, M., Cattoir, S., Battal, C., Occelli, V., Mattioni, S., & Collignon, O. (2020). Shared Representation of Visual and Auditory Motion Directions in the Human Middle-Temporal Cortex. *Current Biology*, *30*(12), 2289-2299.e8. https://doi.org/10.1016/j.cub.2020.04.039

Ricciardi, E., Basso, D., Sani, L., Bonino, D., Vecchi, T., Pietrini, P., & Miniussi, C. (2011). Functional inhibition of the human middle temporal cortex affects non-visual motion perception: A repetitive transcranial magnetic stimulation study during tactile speed discrimination. *Experimental Biology and Medicine*, *236*(2), 138–144. https://doi.org/10.1258/ebm.2010.010230

Ricciardi, E., Vanello, N., Sani, L., Gentili, C., Scilingo, E. P., Landini, L., Guazzelli, M., Bicchi, A., Haxby, J. V., & Pietrini, P. (2007). The Effect of Visual Experience on the

Development of Functional Architecture in hMT+. *Cerebral Cortex*, *17*(12), 2933–2939. https://doi.org/10.1093/cercor/bhm018

Rizzolatti, G., Scandolara, C., Matelli, M., & Gentilucci, M. (1981). Afferent properties of periarcuate neurons in macaque monkeys. I. Somatosensory responses. *Behavioural Brain Research*, *2*(2), 125–146. https://doi.org/10.1016/0166-4328(81)90052-8

Röder, B., Kusmierek, A., Spence, C., & Schicke, T. (2007). Developmental vision determines the reference frame for the multisensory control of action. *Proceedings of the National Academy of Sciences*, *104*(11), 4753–4758. https://doi.org/10.1073/pnas.0607158104

Röder, B., Rösler, F., & Spence, C. (2004). Early Vision Impairs Tactile Perception in the Blind. *Current Biology*, *14*(2), 121–124. https://doi.org/10.1016/j.cub.2003.12.054

Rohe, T., Ehlis, A.-C., & Noppeney, U. (2019). The neural dynamics of hierarchical Bayesian causal inference in multisensory perception. *Nature Communications*, *10*(1), 1907. https://doi.org/10.1038/s41467-019-09664-2

Rohe, T., & Noppeney, U. (2015). Cortical Hierarchies Perform Bayesian Causal Inference in Multisensory Perception. *PLOS Biology*, *13*(2), e1002073. https://doi.org/10.1371/journal.pbio.1002073

Rohe, T., & Noppeney, U. (2016). Distinct Computational Principles Govern Multisensory Integration in Primary Sensory and Association Cortices. *Current Biology*, *26*(4), 509–514. https://doi.org/10.1016/j.cub.2015.12.056

Rolls, E. T., Huang, C.-C., Lin, C.-P., Feng, J., & Joliot, M. (2020). Automated anatomical labelling atlas 3. *NeuroImage*, *206*, 116189. https://doi.org/10.1016/j.neuroimage.2019.116189

Sadaghiani, S., Maier, J. X., & Noppeney, U. (2009). Natural, Metaphoric, and Linguistic Auditory Direction Signals Have Distinct Influences on Visual Motion Processing.

The Journal of Neuroscience, *29*(20), 6490–6499. https://doi.org/10.1523/JNEUROSCI.5437-08.2009

Schneider, M., Kemper, V. G., Emmerling, T. C., De Martino, F., & Goebel, R. (2019). Columnar clusters in the human motion complex reflect consciously perceived motion axis. *Proceedings of the National Academy of Sciences*, *116*(11), 5096–5101. https://doi.org/10.1073/pnas.1814504116

Serino, A., Canzoneri, E., & Avenanti, A. (2011). Fronto-parietal Areas Necessary for a Multisensory Representation of Peripersonal Space in Humans: An rTMS Study. *Journal of Cognitive Neuroscience*, *23*(10), 2956–2967. https://doi.org/10.1162/jocn_a_00006

Soto-Faraco, S., & Azañón, E. (2013). Electrophysiological correlates of tactile remapping. *Neuropsychologia*, *51*(8), 1584–1594. https://doi.org/10.1016/j.neuropsychologia.2013.04.012

Summers, I. R., Francis, S. T., Bowtell, R. W., McGlone, F. P., & Clemence, M. (2009). A functional-magnetic-resonance-imaging investigation of cortical activation from moving vibrotactile stimuli on the fingertip. *The Journal of the Acoustical Society of America*, *125*(2), 1033–1039. https://doi.org/10.1121/1.3056399

Trzcinski, N. K., Hsiao, S. S., Connor, C. E., & Gomez-Ramirez, M. (2023). Multi-finger receptive field properties in primary somatosensory cortex: A revised account of the spatiotemporal integration functions of area 3b. *Cell Reports*, *42*(3), 112176. https://doi.org/10.1016/j.celrep.2023.112176

Van der Stoep, N., & Alais, D. (2020). Motion Perception: Auditory Motion Encoded in a Visual Motion Area. *Current Biology*, *30*(13), R775–R778. https://doi.org/10.1016/j.cub.2020.05.010

van Kemenade, B. M., Seymour, K., Wacker, E., Spitzer, B., Blankenburg, F., & Sterzer, P. (2014). Tactile and visual motion direction processing in hMT+/V5. *NeuroImage*, *84*, 420–427. https://doi.org/10.1016/j.neuroimage.2013.09.004

Vernet, M., Quentin, R., Chanes, L., Mitsumasu, A., & Valero-CabrÃ©, A. (2014). Frontal eye field, where art thou? Anatomy, function, and non-invasive manipulation of frontal regions involved in eye movements and associated cognitive operations. *Frontiers in Integrative Neuroscience*, *8*. https://doi.org/10.3389/fnint.2014.00066

Winkler, A. M., Ridgway, G. R., Douaud, G., Nichols, T. E., & Smith, S. M. (2016). Faster permutation inference in brain imaging. *NeuroImage*, *141*, 502–516. https://doi.org/10.1016/j.neuroimage.2016.05.068

Xu, Y., Vignali, L., Sigismondi, F., Crepaldi, D., Bottini, R., & Collignon, O. (2023). Similar object shape representation encoded in the inferolateral occipitotemporal cortex of sighted and early blind people. *PLOS Biology*, *21*(7), e3001930. https://doi.org/10.1371/journal.pbio.3001930

Zeki, S., Watson, J., Lueck, C., Friston, K., Kennard, C., & Frackowiak, R. (1991). A direct demonstration of functional specialization in human visual cortex. *The Journal of Neuroscience*, *11*(3), 641–649. https://doi.org/10.1523/JNEUROSCI.11-03-00641.1991

Zihl, J., Von Cramon, D., & Mai, N. (1983). SELECTIVE DISTURBANCE OF MOVEMENT VISION AFTER BILATERAL BRAIN DAMAGE. *Brain*, *106*(2), 313–340. https://doi.org/10.1093/brain/106.2.313

Zimmermann, J., Goebel, R., De Martino, F., Van De Moortele, P.-F., Feinberg, D., Adriany, G., Chaimow, D., Shmuel, A., Uğurbil, K., & Yacoub, E. (2011). Mapping the Organization of Axis of Motion Selective Features in Human Area MT Using High-Field fMRI. *PLoS ONE*, *6*(12), e28716. https://doi.org/10.1371/journal.pone.0028716

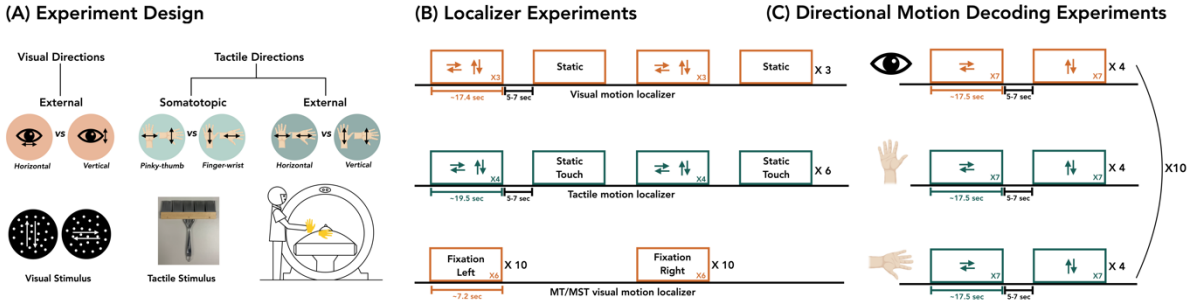

Figure 1. Experiments.

(A) Experiment design. 2 tactile frames of reference X 2 tactile motion directions X 2 visual motion directions. The tactile frames of reference were manipulated using two hand positions - Hand Up and Hand Down. Within each hand position, the tactile stimulation is either along the axis of pinky-thumb or finger-wrist. Thus, with the manipulation of hand postures, the tactile motion directions were either defined somatotopically (pinky-thumb and finger-wrist) or in the external space (horizontal and vertical). The two visual axis-of-motion directions defined in the external space were horizontal and vertical.

(B) Localizer Experiments. Experiments were performed to functionally and individually define the Regions-of-Interest (ROIs). The visual and tactile motion localizers consisting of alternating motion and static stimuli were used to functionally identify visual and tactile motion selective regions respectively. MT/MST visual motion localizer consisting of visual radial motion (approaching and receding) in alternating left and right hemifield was performed to identify MST and MT areas in each individual.

(C) Directional Motion Decoding Experiments. 30 runs were performed with each participant, where each run consisted of only directional motion stimulation. 10 runs corresponded to a single sensory modality and one hand position. One beta map corresponding to each motion direction was obtained from 1 run. Thus, 10 beta maps corresponding to each motion direction, each sensory modality and each hand position were used for Multivariate Pattern Analyses (MVPA).

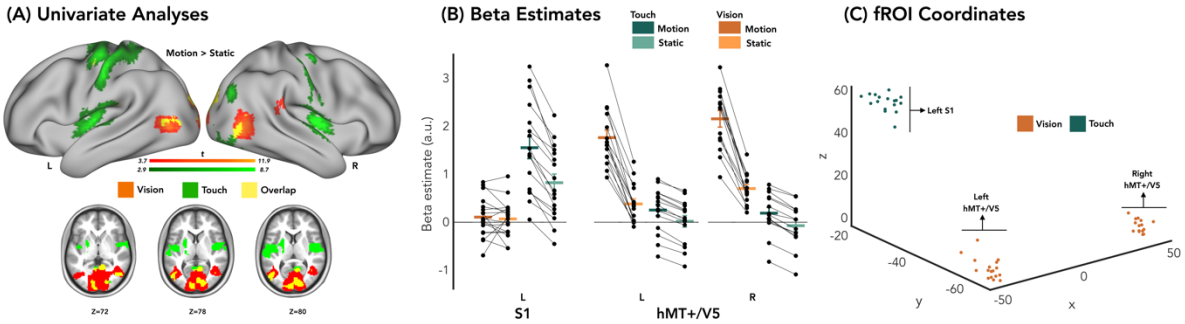

Figure 2. functional Regions-of-Interest (fROIs) and associated univariate activity.

(A) Group-level univariate analyses of visual (orange) and tactile (green) motion > static contrasts. There is an overlap between the visual and tactile motion selectivity in the hMT+/V5 (yellow).

(B) Beta estimates from the visual and tactile motion localizer in each individually-defined fROIs showing visual (orange) and tactile (green) motion selectivity. Tactile beta estimates in hMT+/V5 are from the individually overlapping visual and tactile motion selective response in hMT+/V5. Betas are plotted for illustration purposes only, for statistics please see the appropriate section in the text. Error bars represent the standard error mean

(C) MNI coordinates of the individually-defined spherical functional ROIs.

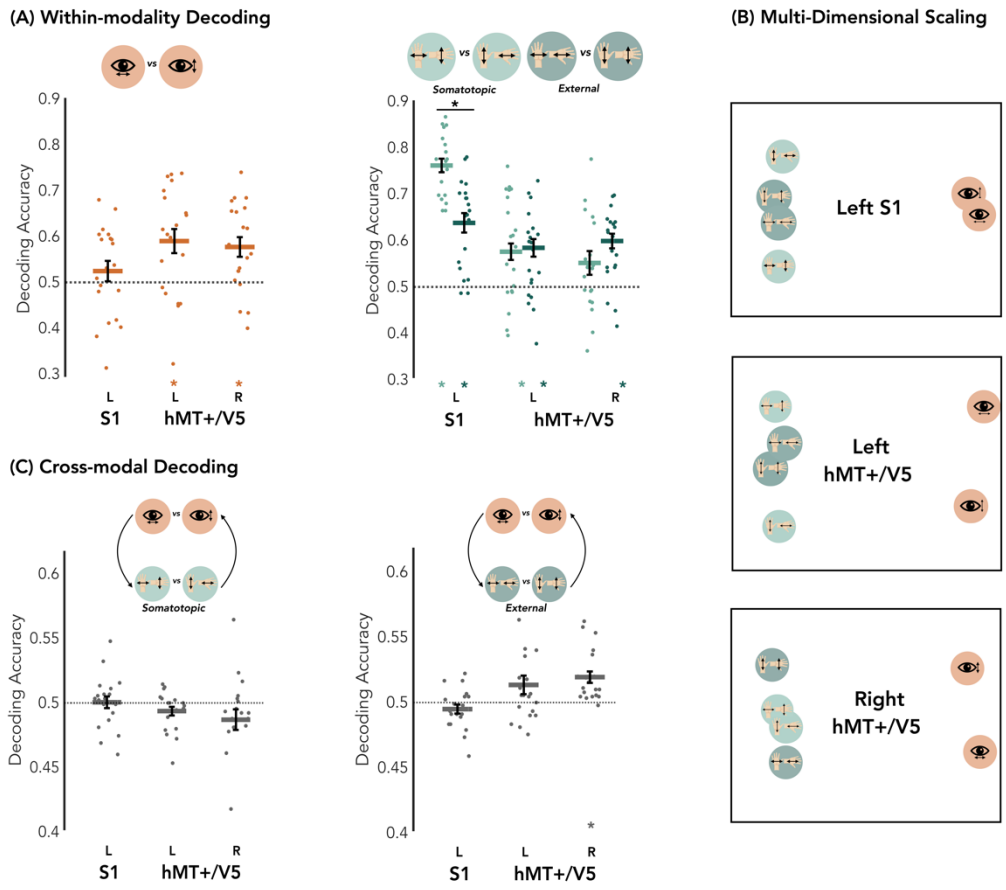

Figure 3. fROI-based MultiVariate Pattern Analyses (MVPA).

(A) Within-Modality Decoding. Binary classification of visual (left panel) and tactile (right panel) motion directions across the two frames of references in each fROI. The y-axis represents the decoding accuracy with chance level at 0.5. Results are FDR corrected (*p<0.05) for the number of fROIs.

(B) Multi-Dimensional Scaling (MDS). Visualisation of the relative distance between the patterns of the visual and tactile motion directions across the two frames of reference in each fROI.

(C) Cross-Modal Decoding. Cross-modal classification between visual and tactile motion directions across the two frames of reference – somatotopic (left panel) and external (right panel) within each fROI. The classifier is trained on visual motion-directions and tested on tactile motion-directions, and vice-versa, with the decoding accuracies subsequently averaged (see supplemental material for each direction separated). Results are FDR corrected (*p<0.05) for the number of ROIs.

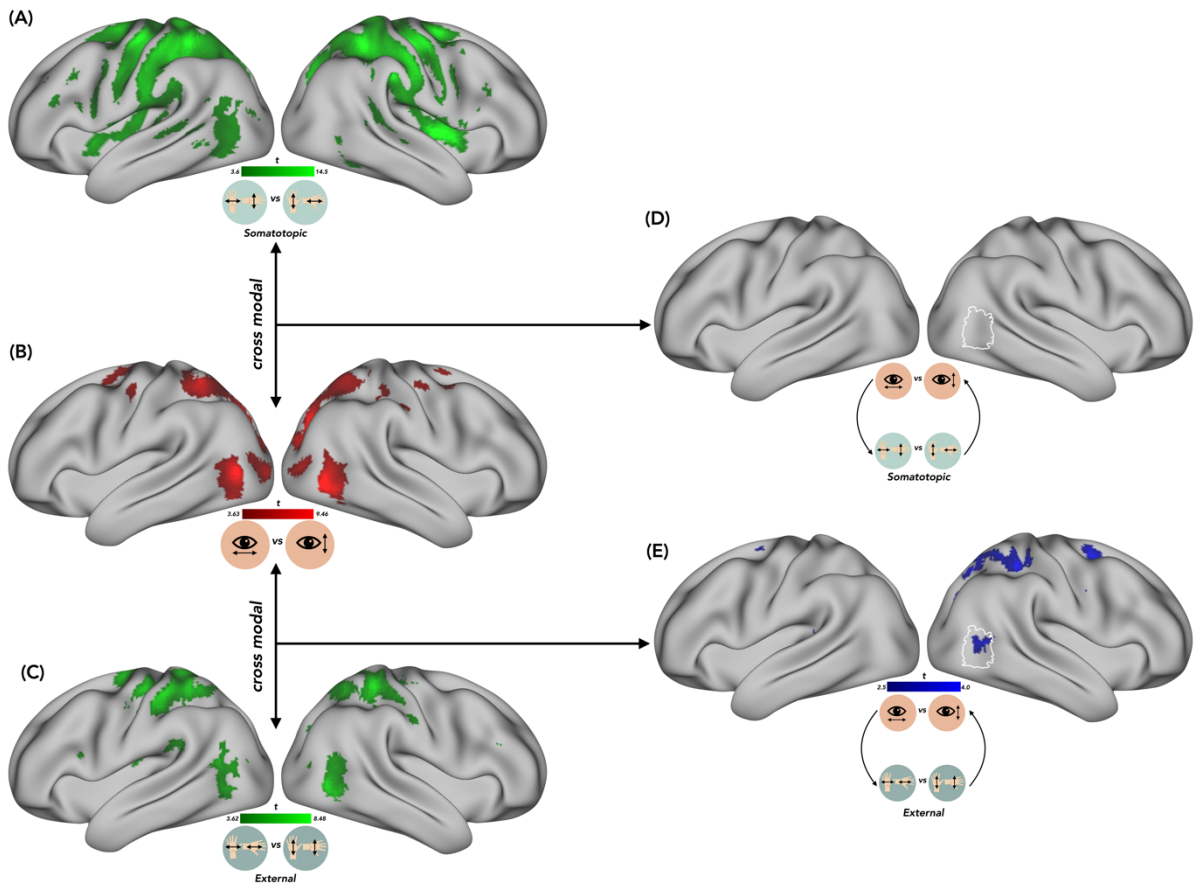

Figure 4. Searchlight Analyses.

(A) Within-modality decoding of tactile motion directions defined in the somatotopic frame of reference.

(B) Within-modality decoding of visual motion directions.

(C) Within-modality decoding of tactile axis-of-motion directions defined in the external frame of reference.

(D) Cross modal decoding between visual and tactile motion directions defined in the somatotopic frame of reference.

(E) Cross modal decoding between visual and tactile motion directions defined in the external frame of reference.

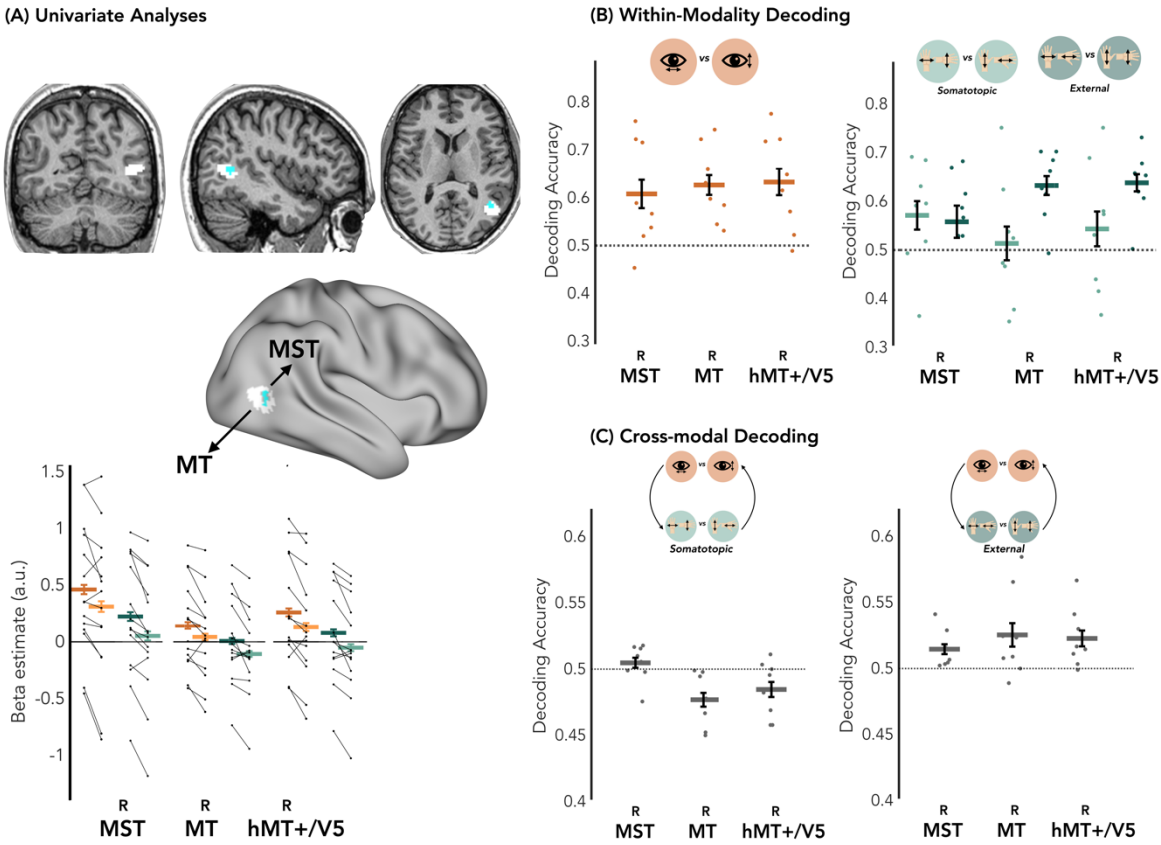

Figure 5. Analyses in the MT/MST.

(A) Univariate Analyses. Example of an individually localized MST and MT from the MT/MST visual motion localizer(top). Beta estimates of visual – motion and static, and tactile – motion and static in the individually localized right MST, right MT and right hMT+/V5 (Below). The MST and MT were identified in 14 out of the 18 tested participants. Table 5 shows the number of voxels in each identified cluster.

(B) Within-modality decoding of visual and tactile motion directions across the two frames of reference in the right MST, MT and hMT+/V5.

(C) Cross-modal decoding between visual and tactile motion directions across the two frames of reference – somatotopic (left panel) and external (right panel) within each ROI. In the left panel, the tactile motion directions are defined in somatotopic frame of reference and in the right panel, the tactile motion directions are defined in the external frame of reference.

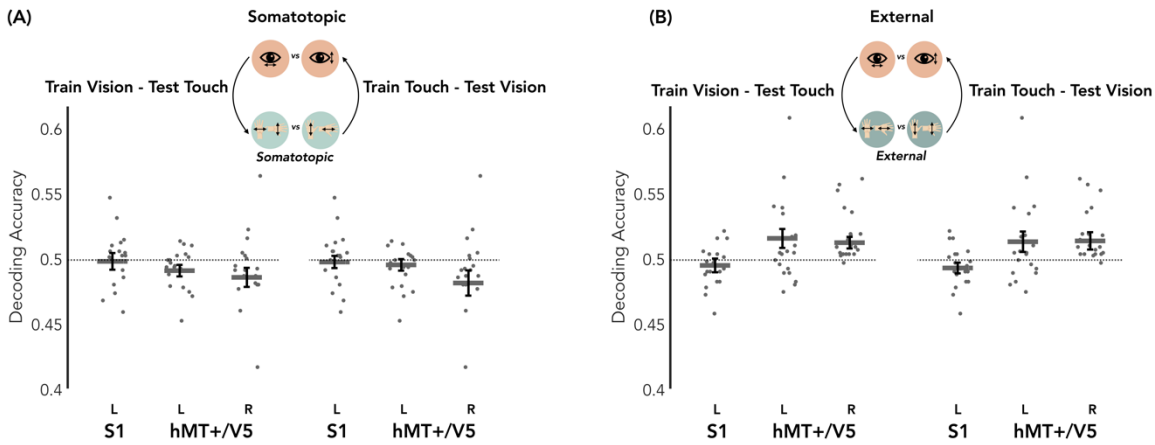

SFigure 1. Cross-Modal Decoding in the ROIs for different directions of train- and test-sets.

(A) Cross-modal classification between visual and tactile motion directions in the somatotopic frame of reference. The left side shows the results when the classifier is trained on visual modality and tested on tactile modality. The right side shows the results when the classifier is trained on tactile modality and tested on visual modality.

(B) Cross-modal classification between visual and tactile motion directions in the external frame of reference. The left side shows the results when the classifier is trained on visual modality and tested on tactile modality. The right side shows the results when the classifier is trained on tactile modality and tested on visual modality.

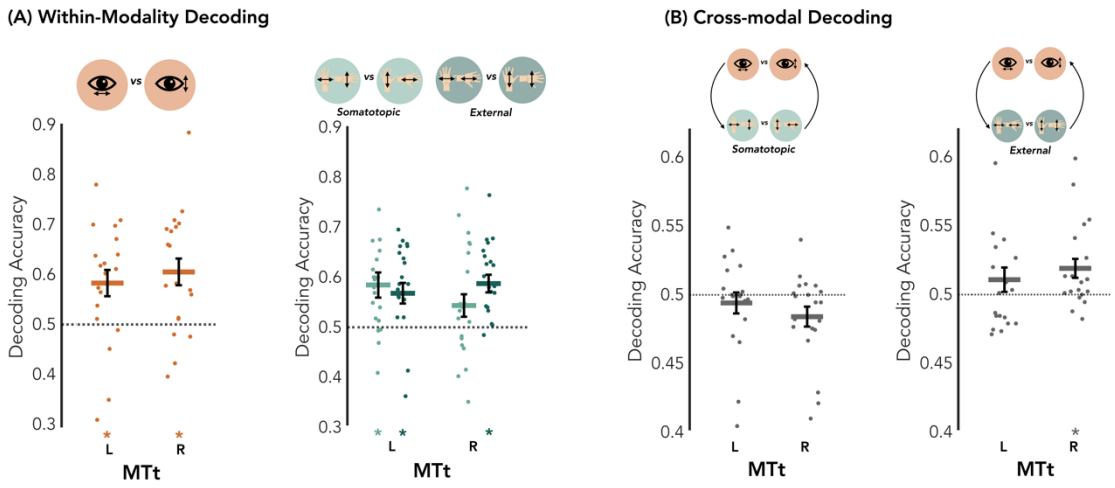

SFigure 2. Multivariate Pattern Analyses in the MTt.

(A) Within-Modality Decoding. Binary classification of visual (left panel) and tactile (right figure) motion directions across the two frames of references in each ROI. The y-axis represents the decoding accuracy, and the chance level is 0.5. (*p<0.05) .

(B) Cross-Modal Decoding. Cross-modal classification between visual and tactile motion directions across the two frames of reference – somatotopic (left panel) and external (right panel) within each ROI. In the left panel, the tactile motion directions are defined in somatotopic frame of reference and in the right panel, the tactile motion directions are defined in the external frame of reference.

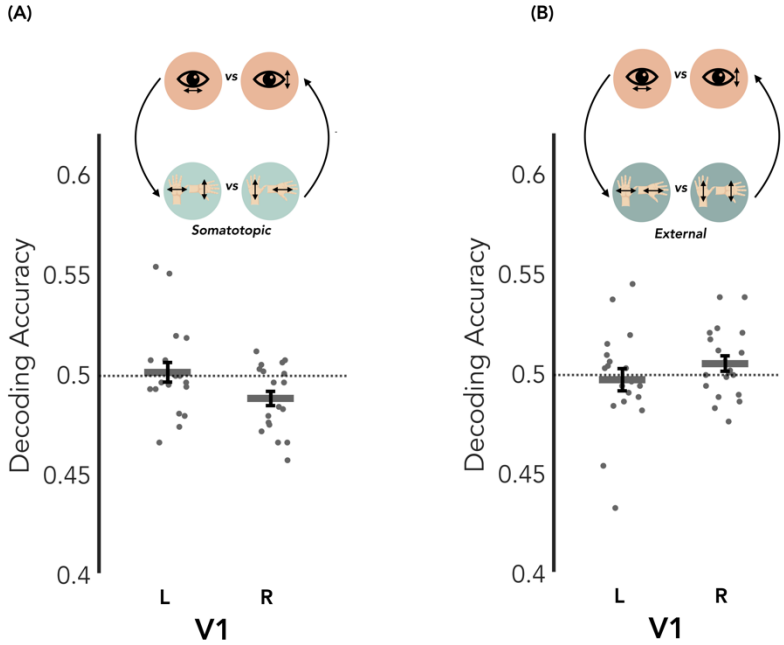

SFigure 3. Cross-Modal Decoding in V1.

A spherical fROI (radius 8mm) of the visual area V1 was defined in each individual using the peak coordinate left V1 [-13, -83, -10 mm] and right V1 [8, -83, -5 mm] observed from the group-level univariate analysis of visual motion localizer (motion > static) (STable 1).

(A) Cross-modal classification between visual and tactile motion directions in the somatotopic frame of reference.

(B) Cross-modal classification between visual and tactile motion directions in the external frame of reference.

Area	K	x(mm)	y(mm)	z(mm)	Z	T	p(FWE-corr)
L Superior Occipital G (V3A)	1272	-10	-99	8	6.7	15.36	0
R Lingual G (V1)		8	-83	-5	6.55	14.42	0
L Lingual G (V1)		-13	-83	-10	6.24	12.69	0
L Middle Temporal G (hMT+/V5)	12	-47	-70	5	5.09	8	0.014
R Middle Temporal G (hMT+/V5)	4	47	-65	3	4.83	7.24	0.039

STable 1. Whole-brain univariate analysis results from the visual motion localizer (visual motion > static). Results are corrected for multiple comparisons using family-wise error (FWE) correction across the whole brain at a significance level of $p < 0.05$. Coordinates are reported in MNI space, and regions are identified using the Automated Anatomical Labeling (AAL) atlas. L: Left; R: Right.

Area	K	x(mm)	y(mm)	z(mm)	Z	T	p(FWE-corr)
L Postcentral G (S1)	4312	-55	-21	52	5.29	8.65	0.005
L Postcentral G		-44	-26	63	5.19	8.33	0.007
L Rolandic Oper (S2)		-42	-16	13	4.97	7.66	0.017
R Insula (S2)	1149	39	-8	11	4.32	5.95	0.18
L Middle Temporal G (hMT+/V5)	104	-52	-70	8	3.19	3.8	0.026*
R Middle Temporal G (hMT+/V5)	122	-52	-42	-10	2.98	3.47	0.043*

STable 2. Whole-brain univariate analysis results from the tactile motion localizer. Results are corrected for multiple comparisons using family-wise error (FWE) correction across the whole brain at $p < 0.05$ or within small spherical volumes (*). Coordinates are reported in MNI space. Coordinates for small volume correction were derived from the independent visual motion localizer [MNI coordinates for left hMT+/V5: -47, -70, 5; right hMT+/V5: 47, -65, 3]. Regions are identified using the Automated Anatomical Labeling (AAL) atlas. L: Left; R: Right.

Searchlight decoding	Hemisphere	Area	SVC p-value
Visual Directions	left	hMT+/V5	0
	right	hMT+/V5	0
	left	Intraparietal Area	0
	right	Intraparietal Area	0
Tactile directions in the somatotopic frame of reference	left	hMT+/V5	0
	right	hMT+/V5	0.024
	left	Intraparietal Area	0
	right	Intraparietal Area	0.001
Tactile directions in the external frame of reference	left	hMT+/V5	0.010
	right	hMT+/V5	0
	left	Intraparietal Area	0
	right	Intraparietal Area	0.020
Cross-modal decoding of visual and tactile directions in the somatotopic frame of reference	left	hMT+/V5	no clusters
	right	hMT+/V5	no clusters
	left	Intraparietal Area	no clusters
	right	Intraparietal Area	no clusters
Cross-modal decoding of visual and tactile directions in the external frame of reference	left	hMT+/V5	no clusters
	right	hMT+/V5	0.031
	left	Intraparietal Area	no clusters
	right	Intraparietal Area	0.031
	left	Frontal Area	no clusters
	right	Frontal Area	0.008

STable 3. Summary Statistics of Searchlight Decoding. Small Volume Correction (SVC) was applied at the independently identified locations of left hMT+/V5 (-47, -70, 5 mm) and right hMT+/V5 (47, -65, 3 mm) from the visual motion localizer. Additionally, SVC was applied to parietal regions using coordinates from a prior study (Summers et al., 2009) that evaluated tactile motion selectivity [moving tactile > stationary tactile]: left Intraparietal Area (Talairach: -30, -50, 45; MNI: -30, -53, 49 mm) and right Intraparietal Area (Talairach: 42, -51, 49; MNI: 41, -55, 54 mm) and frontal regions using coordinates from a previous study (Lloyd et al., 2003) investigating the external representation of touch : left dorsal prefrontal crotex (-46, 8, 46 mm) and right dorsal prefrontal cortex (24, 4, 58 mm).

Experiment	Condition	N	mean	SD	SEM
Visual Motion Localizer	Motion	18	0.824	0.381	0.09
Visual Motion Localizer	Static	18	0.824	0.381	0.09
Tactile Motion Localizer	Motion	18	0.72	0.403	0.095
Tactile Motion Localizer	Static	18	0.731	0.409	0.096
MT/MST Localizer	Motion-Left	18	0.9	0.293	0.069
MT/MST Localizer	Motion-Right	18	0.861	0.318	0.075
Visual	Vertical	20	0.935	0.124	0.028
Visual	Horizontal	20	0.921	0.125	0.028
Hand Up	Pinky-Thumb	20	0.874	0.144	0.032
Hand Up	Finger-Wrist	20	0.863	0.149	0.033
Hand Down	Pinky-Thumb	20	0.864	0.187	0.042
Hand Down	Finger-Wrist	20	0.835	0.195	0.044

STable 4. Behavioral performance across experimental conditions. N is the number of participants; mean is the mean performance accuracy calculated across participants; SD is the standard deviation; SEM is the standard error mean.

	lS1	lhMT+/V5	rhMT+/V5
S1	-36.40, -28.80, 57.40	-49.40, -57.40, 8.0	49.38, -64.79, 5.37
S2	-44.33, -28.09, 54.98	-41.57, -58.37, 12.72	46.63, -61.12, 5.37
S3	-42.49, -21.67, 58.66	-46.17, -64.79, 3.53	46.80, -62.60, 0.20
S4	-42.49, -30.85, 55.90	-43.41, -66.63, 9.04	46.63, -60.21, 2.61
S5	-39.74, -26.26, 58.66	-46.17, -60.21, 5.37	45.71, -58.37, 6.29
S6	-39.0,-26.20, 62.60	-44.33, -64.79, 2.61	43.87, -61.12, -0.15
S7	-44.33, -19.84, 56.82	-46.80, -67.80, 2.80	48.47, -62.04, 0.20
S8	-41.60, -24.42, 58.66	-46.17, -66.63, 0.20	46.80, -60.21, 4.45
S9	-38.90, -28.09, 58.66	-44.33, -66.63, 8.12	45.71, -62.04, 0.20
S10	-37.90, -28.09, 58.66	-44.33, -66.63, 5.37	45.71, -62.04, 2.61
S11	-39.0, -28.09, 56.82	x	x
S12	-42.49, -24.42, 56.82	-48.01, -67.55, 5.40	x
S13	-42.49, -23.60, 59.57	-44.33, -64.79, -0.15	49.40, -61.12, -2.90
S14	-44.33, -28.09, 55.90	-42.49, -66.63, 1.69	46.80, -62.96, -1.06
S15	-43.41, -22.59, 54.98	-46.80, -65.20, 0.20	46.63, -60.21, 2.61
S16	-44.20, -31.40, 49.60	-44.20, -67.80, 0.20	45.71, -62.04, -0.15
S17	x	x	x
S18	x	x	x
S19	-39.0, -28.09, 56.82	-49.40, -62.60, 2.80	54.60, -57.40, 0.20
S20	-35.14, -28.09, 59.57	-49.40, -65.20, 2.80	45.71, -62.96, 3.53

STable 5. MNI Coordinates of the individually defined regions of interest (ROIs). Coordinates of bilateral hMT+/V5 were defined in each subject from the contrast [visual motion > visual static] in the visual motion localizer. Coordinates of left S1 were defined in each subject from the contrast [tactile motion > tactile static] in the tactile motion localizer.

Subject	Right hMT+/V5	Right MST	Right MT
S1	192	16	176
S2	312	133	179
S3	243	10	233
S4	306	212	94
S5	190	21	169
S6	270	112	158
S7	208	10	198
S8	305	40	265
S9	298	52	246
S10	301	134	167
S11	-	-	-
S12	-	-	-
S13	164	-	-
S14	367	34	333
S15	440	110	330
S16	344	4	340
S17	x	x	x
S18	x	x	x
S19	58	21	37
S20	379	11	368

STable 6. Voxel counts in the right hemisphere hMT+/V5 complex and its subregions – MST and MT. Number of voxels within each region of interest (ROI): right hemisphere hMT+/V5, MST, and MT. X denotes participants not tested for MT/MST visual motion localizer. – denotes that there were no clusters observed.

Subject	Left Hemisphere	Right Hemisphere
S1	0.669354839	0.798319328
S2	0.065306122	0.359832636
S3	0.186234818	0.260162602
S4	0.21399177	0.333333333
S5	0	0.348178138
S6	0.551440329	0.123966942
S7	0.048780488	0.11814346
S8	0.721311475	0.533333333
S9	0.202531646	0.271604938
S10	0.878661088	0.685714286
S11	0.596774194	0.205761317
S12	0.468619247	0.205761317
S13	0.040983607	0.226720648
S14	0.04	0.193277311
S15	0.227642276	0.216666667
S16	0.696721311	0.721311475
S17	0.596774194	0.205761317
S18	0.596774194	0.205761317
S19	0.596774194	0.205761317
S20	0.308943089	0.545454545

STable 7. Dice Coefficient between the individually localized hMT+/V5 and MTt. The dice coefficient depicts the spatial overlap between individually localized hMT+/V5 and MT regions within each participant.